LYSIMETER MEASUREMENTS OF SALAL UNDERSTORY EVAPOTRANSPIRATION AND FOREST SOIL EVAPORATION AFTER SALAL REMOVAL IN A DOUGLAS-FIR PLANTATION

by

PETER MARTIN OSBERG

B.S.F., University of British Columbia, 1983

A THESIS SUBMITTED IN PARTIAL FULFILLMENT OF

THE REQUIREMENTS FOR THE DEGREE OF

MASTER OF SCIENCE

in

THE FACULTY OF GRADUATE STUDIES

Department of Soil Science

We accept this thesis as conforming

to the required standard

THE UNIVERSITY OF BRITISH COLUMBIA

March 1986

In presenting this thesis in partial fulfilment of the requirements for an advanced degree at the University of British Columbia, I agree that the Library shall make it freely available for reference and study. I further agree that permission for extensive copying of this thesis for scholarly purposes may be granted by the head of my department or by his or her representatives. It is understood that copying or publication of this thesis for financial gain shall not be allowed without my written permission.

Department of Soil Science

The University of British Columbia
2075 Wesbrook Place
Vancouver, Canada
V6T 1W5

Date April 14, 1986

ABSTRACT

Two weighing lysimeters were constructed in a 23-year-old Douglas-fir (Pseudotsuga menziesii (Mirb.) Franco) stand. The salal (Gaultheria shallon Pursh.) understory was mechanically removed from a 30 x 40 m plot and one lysimeter was located at the center of this plot to measure daily forest soil evaporation (E_s). For 8 consecutive days, in August 1984, E_s ranged between 0.08 and 0.34 mm d^{-1} which was 15-18% of the daily total stand evapotranspiration. In July 1985, after removing salal from the second lysimeter, which was positioned under a less dense tree canopy, E_s was 0.34 - 0.41 mm d^{-1} which was 17-21% of the daily whole stand evapotranspiration. Forest floor diffusive resistances (r_{co}), computed by rearranging the Penman-Monteith equation, were found to range between 900 and 3500 s m^{-1}.

The measured daily evapotranspiration rate from the understory (E_t) with salal present was 0.60 - 0.84 mm d^{-1}, which was equivalent to 30-42% of the daily stand evapotranspiration.

The dependence on windspeed of the bulk aerodynamic resistance (s m^{-1}) to vapour transport (r_A) between the salal canopy and measurement height (0.3 m above the top of the salal canopy) was found to be $r_A = 25.2\ \bar{u}^{-0.554}$, where $\bar{u}$ is the mean windspeed (m s^{-1}) at measurement height. Approximately 70-75% of r_A was estimated to be attributable to the leaf boundary-layer resistance. The evaporation rate from wet foliage was found to be 5 times greater than the transpiration rate from dry foliage exposed to similar meteorological conditions.

Analysis of the relative importance of net available energy flux density and advective processes in determining the latent heat flux density from the understory yielded a range of Ω values between 0.15 and 0.22. The vapour pressure deficit below the tree canopy was found to be largely determined by the vapour pressure deficit above the tree canopy, with very little local adjustment.

TABLE OF CONTENTS

LIST OF FIGURES

LIST OF TABLES

NOTATION

A_a	available energy above the tree canopy (i.e., Rn-G) (W m^{-2})
A_b	available energy below the tree canopy (W m^{-2})
C	volumetric heat capacity of soil (J m^{-3} $°C^{-1}$)
D	atmospheric vapour pressure deficit (kPa)
D_{eq}	equilibrium atmospheric vapour pressure deficit (kPa) defined by equation (28)
D_i	atmospheric vapour pressure deficit just above layer i (kPa)
D_{i-1}	atmospheric vapour pressure deficit just above layer i-1 (kPa)
D_m	atmospheric vapour pressure deficit at a reference height within the well mixed portion of the planetary boundary layer (kPa)
D_o	atmospheric vapour pressure deficit within the canopy at a level considered to be an effective source height (kPa)
E_d	transpiration rate of dry foliage (mm $period^{-1}$)
E_{eq}	equilibrium evapotranspiration rate (mm $period^{-1}$)
E'	calculated transpiration rate from the understory salal (mm $period^{-1}$)
E_s	forest soil evaporation rate (mm $period^{-1}$)
E_t	total understory evapotranspiration (i.e., vegetation transpiration + soil evaporation) (mm $period^{-1}$)
E_w	evaporation rate of intercepted water (mm $period^{-1}$)
F_{BS}	force of the bottom spring (N)
F_{cw}	force of the counterweights (N)
F_{lys}	downward force of the lysimeter (N) (mass of the lysimeter multiplied by the acceleration of gravity)

F_s	shade factor
F_{TS}	force of the top spring (N)
G	soil heat flux density (W m^{-2})
G_5	soil heat flux density at the 5 cm depth (W m^{-2})
G_0	soil heat flux density at the surface (W m^{-2})
L	latent heat of vaporization of water (J kg^{-1})
LA	leaf area (m^2)
LA1	measured leaf area of a small subsample (m^2)
LAI	leaf area index on a one-sided basis (m^2 m^{-2})
LAI_i	leaf area index on a one-sided basis for layer i (m^2 m^{-2})
LE	latent heat flux density (W m^{-2})
LE_{i-1}	latent heat flux density above layer i-1 (W m^{-2})
LE'_i	calculated latent heat flux originating from layer i (W m^{-2})
M	rate of change of soil heat storage in the soil above the heat flux plates (W m^{-2})
ML	mass of leaves (g)
MT	mass of twigs (g)
M2	mass of larger foliage subsample (g)
P	precipitation (mm $period^{-1}$)
Rn	net radiation flux density (W m^{-2})
Rn_i	net radiation flux density above layer i (W m^{-2})
Rn_{i-1}	net radiation flux density above layer i-1 (W m^{-2})
S_t	solar irradiance (W m^{-2})

T	air temperature (°C)
T_0	air temperature at the beginning of a lysimeter measurement period (°C)
V_{BAL}	LVDT output voltage when the lysimeter is balanced (mV)
V_{LVDT}	LVDT output voltage (mV)
W_d	depth of water in the lysimeter (mm)
W_c	water content of the fine soil fraction (i.e., < 2 mm fraction) kg kg^{-1})
W_{ref}	depth of water in the lysimeter at the beginning of a measurement period (mm)
Z	depth of soil (m)
c	30 second count while the neutron probe is positioned at a depth in the soil
c_p	specific heat of moist air (J kg^{-1} $°C^{-1}$)
c_s	30 second count while the neutron probe is contained within the shield (i.e., standard counts)
d	average salal leaf diameter (m)
d_{cw}	distance between the point of attachment of the counterweights to the suspension beam and the fulcrum (m)
d_{lys}	distance between the point of attachment of the lysimeter to the suspension beam and the fulcrum (m)
d_{LVDT}	distance between the point of contact of the LVDT probe on the suspension beam and the fulcrum (m)
d_s	distance between the point of attachment of the springs to the suspension beam and the fulcrum (m)
f	volumetric stone fraction on a whole soil basis
k	spring constant (g cm^{-1})
k'	lysimeter calibration factor (i.e., reciprocal of sensitivity (mm mV^{-1})

m	the temperature sensitivity of the modulus of rigidity ($°C^{-1}$)
r	radius of the lysimeter (m)
r_A	bulk aerodynamic resistance to vapour transport from the salal canopy to the meteorological sensors ($s\ m^{-1}$)
r_{Ai}	bulk aerodynamic resistance to vapour transport from layer i to the meteorological sensor height ($s\ m^{-1}$)
r_{ai}	eddy diffusive resistance to sensible and latent heat flux above layer i ($s\ m^{-1}$)
r_{as}	eddy diffusive resistance to vapour transport from the surface to a reference height in the well mixed portion of the planetary boundary-layer ($s\ m^{-1}$)
r_b	boundary-layer resistance to sensible and latent heat flux ($s\ m^{-1}$)
r_{bi}	boundary-layer resistance to sensible and latent heat flux on a one-sided leaf area basis for layer i ($s\ m^{-1}$)
r_c	mean canopy resistance to latent heat flux ($s\ m^{-1}$)
r_{ci}	mean canopy resistance to latent heat flux for layer i ($s\ m^{-1}$)
r_{co}	forest floor diffusive resistance to latent heat flux ($s\ m^{-1}$)
r_c^*	critical canopy resistance ($s\ m^{-1}$)
r_H	leaf boundary-layer resistance to sensible heat flux on one side ($s\ m^{-1}$)
r_{Ha}	average canopy leaf boundary layer resistance to sensible heat flux ($s\ m^{-1}$)
r_{Hi}	leaf boundary-layer resistance to sensible heat flux on one side for layer i ($s\ m^{-1}$)
r_s	stomatal resistance to latent heat flux of one side of a hypostomatous leaf ($s\ m^{-1}$)
r_{si}	stomatal resistance to latent heat flux of one side for layer i ($s\ m^{-1}$)

r_v	boundary-layer resistance to latent heat flux of one side of a leaf (s m^{-1})
r_{va}	average canopy boundary-layer resistance to latent heat flux (s m^{-1})
r_{vi}	boundary-layer resistance to latent heat flux of one side of a leaf for layer i (s m^{-1})
s	slope of the saturated vapour pressure curve (kPa $°C^{-1}$)
t	time (s)
$\bar{u}$	mean windspeed (s m^{-1})
X_B	elongation of the bottom spring (cm)
X_{LVDT}	displacement of the LVDT probe (cm)
X_s	elongation of the top and bottom springs (cm)
X_T	elongation of the top spring (cm)
γ	psychrometric constant (kPa $°C^{-1}$)
δ_i	term in equation (6) to account for the net radiation and latent heat flux densities below layer i in determining the latent heat flux from layer i (kPa) (defined by equation (7))
θ_v	whole soil volumetric water content (m^3 m^{-3})
ρ	density of moist air (kg m^{-3})
ρ_{fs}	bulk density of the fine soil (< 2 mm) fraction (kg m^{-3})
ρ_w	density of liquid water (kg m^{-3})
Ω	weighting factor defined by equation (30)

ACKNOWLEDGEMENTS

I am very thankful for the tremendous support and encouragement I received from my family and friends, most notably Marion Osberg, Peter Chapman, Lyle Osberg, Candace Morgan, Ian MacDonald, and John Robertson.

I wish to express my sincere appreciation to Dr. T.A. Black, my academic supervisor, for unreservedly sharing his wealth of experience and knowledge with me. I am also very grateful for his continuous financial support throughout the duration of my graduate studies.

I wish to thank the other members of my academic committee, Dr. T.M. Ballard, Dr. M.D. Novak, and Dr. D.L. Spittlehouse, for their assistance in problem definition and suggestions on sampling procedures and analytical approaches.

Don Giles and Dave Price deserve a special note of thanks for their significant assistance in conducting the field work, and for their much appreciated moral support when it looked as though my iron artistry would never swing.

My ability to conduct this research was greatly enhanced by the daily intellectual stimulation and friendship I received from Nigel Livingston, Bob Stathers, Doug Beames, and Dr. Frank Kelliher.

I wish to thank B.C. Forest Products Ltd. for their financial support through the B.C.F.P. Graduate Student Fellowship in Soil Science.

The financial and material support, for this research, received from, MacMillan Bloedel Ltd., Woodland Services Division, the B.C. Ministry of Forests, the Natural Science and Engineering Research Council, and Ellett Copper and Brass Co. Ltd., was greatly appreciated.

1. INTRODUCTION

The depletion of the old growth coniferous forests of British Columbia and their subsequent replacement with managed plantations has shifted the responsibilities of foresters from those associated with engineering and harvesting to the more biological problems of growing the next crop. The old growth stands currently being harvested from coastal forests contain very large timber volumes, per unit of land area, because the biomass has been accumulating for a long time. Managed plantations will be harvested at an earlier stage of stand development and consequently the accumulated timber volume at the time of the next harvest will be substantially reduced. This reduction in timber volume per hectare will create timber supply shortages in some forest districts in the next ten to twenty years, assuming that the forest will be managed to provide a balanced distribution of maturing age classes (Anon 1980). Private forest firms have already experienced severe reductions in the supply of certain timber species and grades which has resulted in an inability to maintain milling operations at a profitable level. Forest managers, in an attempt to minimize current and projected timber supply shortages, have recommended that silvicultural activities be intensified and that the existing accumulated biomass be more completely utilized (Ainscough 1981).

The objective of intensive silviculture is to grow the maximum volume, of the desired species, on the least number of stems, in the

shortest period of time possible. The success of silvicultural operations in improving stand productivity depends on their effect on the site energy regime, nutrient availability, moisture regime, and soil physical properties. Controlling stand density, through precommercial thinning or juvenile spacing and commercial thinning operations, often results in increased growth rates for the remaining crop trees because the competition between trees for available energy, nutrients, and water is reduced (Daniel et al. 1979; Smith 1962).

Thinning stands shifts the growth capacity of the site to fewer trees which will therefore reach harvestable size in a shorter period of time. The possible benefits of reduced rotation age, reduced harvesting costs, larger individual piece size, higher quality timber, better species mix, and opportunities for small yields midway through the rotation, have generated a lot of interest in thinning second growth stands (Fries and Hagner 1970).

Another strong incentive for forest firms considering investments in thinning juvenile stands is in Section 52 of the British Columbia Forest Act. This section provides for increases in the current annual allowable cut in response to increases in forest productivity achieved through the application of more intensive silviculture (Forest Act 1979). The immediate increase in allowable cut means that the return on investment does not have to be discounted over long periods of time, unlike investment in planting, which is considered to be basic silviculture, and is not eligible for Section 52 consideration.

Thinning is an expensive silvicultural operation and the expense can become prohibitive if the stand must be entered frequently.

Consequently, the tendency has been for silviculturists to prescribe a juvenile spacing early in the rotation followed by a single commercial thinning midway through the rotation, leaving just the number of stems desired at the culmination of the rotation. This sequence of treatments will not decrease the final harvestable timber volume if the residual stand density is sufficient to fully utilize all available resources on the site. If the stand is thinned to a density below that which represents full site occupancy then some of the productive capacity of the site may be shifted to understory shrubs, and the final harvestable timber volume will be reduced.

Jackson et al. (1983) in an investigation of the causes of the poor growth response of Pinus radiata D. Don, planted on deep sand, found that thinning greatly reduced depletion of available soil water, but only for a period of two to three years, by which time full canopy closure had been attained. The application of fertilizer to the stand at the time of thinning increased volume production sixty to seventy percent over that of the control stand. Black et al. (1980) found that thinning a young Douglas-fir (Pseudotsuga menziesii (Mirb.) Franco) plantation, growing on a droughty site but not displaying any signs of nutrient deficiency, resulted in a poor growth response by the remaining crop trees. Salal (Gaultheria shallon Pursh.), growing as an understory shrub in the thinned stand, was considered to be competing for the limited amount of available soil water. Utilizing a procedure which combined water balance measurements of stand evapotranspiration with a simple vapour diffusion model, which required periodic stomatal

conductance measurements for both the trees and the salal, they estimated that as the fraction of extractable soil water decreased from 0.8 to 0.2 the fraction of total transpiration originating from the salal understory, in the thinned stand, increased from forty percent to sixty-five percent. The transpiration rate of trees in the thinned stand was found to be very similar to that of trees in a nearby unthinned stand.

Roberts et al. (1980) measured transpiration from a 50 year old Scots pine (Pinus sylvestris L.) plantation, with an understory of bracken fern (Pteridium aquilinum L.), and found that, for the summer period from June to July, the fraction of total stand transpiration originating from the bracken fern increased from twenty-one percent to fifty-seven percent.

In a study comparing the transpiration from a stand of Scots pine with bracken fern in the understory and a denser stand of Corsican pine (Pinus nigra var. maritima) Roberts et al. (1982) found that the total stand transpiration was very similar but that the transpiration from the Corsican pine trees was 28% greater than from the Scots pine trees. Further investigations by Roberts et al. (1984) showed that the stomatal resistance of the bracken fern understory was less sensitive than that of the Scots pine trees to increases in vapour pressure deficits, and that this resulted in an increase in the contribution, by bracken fern, to the total stand transpiration.

Tan et al. (1977) investigated the relationship of the stomatal resistance to vapour diffusion exerted by Douglas-fir and salal to soil water potential and atmospheric vapour pressure deficit. They showed

that, as the soil water potential decreased, the stomatal resistance of Douglas-fir increased more rapidly than did that of the salal, in response to increased vapour pressure deficits. Using the Penman-Monteith equation, in a growing season water balance model, to partition the total stand evapotranspiration between the Douglas-fir and salal canopies, Spittlehouse and Black (1982) estimated that salal transpired 33% of the available soil water over the growing season. The stomatal resistance characteristics for the two canopies were determined as functions of vapour pressure deficit, root zone water potential, and solar irradiance. The leaf boundary-layer resistance to vapour diffusion was calculated using an equation for flat plates in parallel turbulent flow. Black and Spittlehouse (1981) suggested that thinning stands which experience periodic growing season water deficits may shift water use from the overstory trees to the understory shrubs.

Stewart (1984) presented calculations which demonstrated that the transpiration from tall vegetation is nearly twice as sensitive to increases in stomatal resistance as that from short vegetation. He suggested that, for short vegetation, a reduction in transpiration by stomatal closure will result in an increase in leaf temperature, due to the large aerodynamic resistance to sensible heat flux, and consequently, the vapour pressure gradient, from the substomatal cavities of leaves to the air surrounding the leaves, increases, offsetting the initial reduction in transpiration. Stewart (1984) also suggested that the turbulence generated by tall, rough, forest canopies results in a high rate of exchange between the forest and the

atmosphere, and that as a result of this effective mixing, understory vegetation is likely to be exposed to atmospheric vapour pressure deficits of similar magnitude to those that develop at the tree crown level, and will therefore make a significant contribution to the total stand transpiration.

McNaughton and Jarvis (1983) considered the question of transpiration from understory vegetation and suggested that a dense tree canopy may decouple the air above the understory vegetation from the relatively dry air above the tree canopy. They suggested that this could result in the establishment of an equilibrium vapour pressure deficit, which would be determined by the understory canopy resistance to vapour diffusion and the available energy flux density below the upper canopy; in which case, the transpiration from the understory vegetation would tend to approach the equilibrium transpiration rate and would be determined by the available energy.

Zahner (1958) found that removing the hardwood understory from loblolly (Pinus taeda L.) and shortleaf (Pinus echinata Mill.) pine stands, growing on sandy, upland soils, with a root zone depth of 2 metres, resulted in a reduced rate of soil water depletion during the early part of the growing season and an increase in the root zone volumetric water content of 0.04 m^3 m^{-3}, over stands where the understory vegetation had not been removed.

Kelliher (1985) examined the effect of removing the salal understory from a heavily thinned, 31-year-old Douglas-fir stand, on the root zone water balance. The treatment was confined to pairs of trees

with root zones isolated by trenching down to bedrock. He found that the differences in the root zone water content, throughout the growing season, were small. He used small lysimeters and porometer measurements in combination with a vapour diffusion model to estimate the contributions to total evapotranspiration by the Douglas-fir canopy, salal understory, and the forest floor. He estimated the salal transpiration to be 0.5 to 1.0 mm d^{-1} greater than the forest floor evaporation where salal had been removed. For modelling the salal transpiration he used a value for the leaf boundary-layer resistance which was determined from the relationship between leaf boundary-layer resistance and windspeed developed by Spittlehouse and Black (1982), for artificial salal leaves, and he included a shelter factor of 2, following Thom (1971), to take into consideration the effect of leaf overlap on the boundary-layer resistance to vapour diffusion.

Price et al. (1985) measured the stomatal conductance and photosynthetic rate of Douglas-fir trees growing on plots with the salal understory removed and present. They found that removing salal increased both the stomatal conductance and the photosynthetic capacity of the Douglas-fir leaves. They suggested that, while removing the salal resulted in only very small differences in the root zone water content, these small differences resulted in significantly higher soil water potentials due to the steepness of the soil water retention curve, for sandy loam soil, at low water contents.

The physical principles underlying the micrometeorological methods of estimating evapotranspiration from vegetated surfaces have been

reviewed by Tanner (1968), Thom (1975), and Garratt (1984). The combination methods, which are all based on the Penman-Monteith equation, are generally considered to be the most useful transpiration models currently available because they combine the physics and physiology of evaporation from vegetation with the transfer of water vapour in the atmosphere (Jarvis et al. 1981; Stewart 1983). The combination method has been shown to be very sensitive to the values input for stomatal resistance, which for extensive vegetated surfaces must be considered as a mean canopy resistance, and this parameter has been found to be extremely variable, especially for tree canopies which present the added complication of requiring an estimate of the effective leaf area index (Leverenz et al. 1982; Milne et al. 1985; Aston 1984) actually contributing to transpiration.

This is not as serious a problem for salal because Tan et al. (1977) have shown that the stomatal resistance of salal is not as sensitive to changes in vapour pressure deficit as is Douglas-fir and this tends to confine the range of any variability in stomatal resistance during the day. Furthermore, Milne et al. (1985) pointed out that some of the variability may have been due to the inherent difficulties in measuring the stomatal resistance of conifer needles, whereas, porometer measurements on salal leaves are easy to conduct.

Shuttleworth (1978; 1979) developed a one-dimensional model of evapotranspiration from partially wet forest canopies by applying the Penman-Monteith equation to distinct layers within the canopy. Kelliher (1985) modified the Shuttleworth multilayer model for use in

hypostomatous canopies and used it in combination with a root zone water balance model to examine the effects of salal understory removal on Douglas-fir transpiration rates. The canopy resistance functions were modelled using relationships proposed by Tan et al. (1978) and Spittlehouse and Black (1982), and the aerodynamic resistance to turbulent transport was estimated, following Thom (1975), by assuming an exponential eddy diffusivity profile from the top of the trees to the salal canopy.

While some researchers have questioned the validity of using flux-gradient relationships to model the turbulent transport of vapour within plant canopies (Bradley et al. 1983; Denmead 1984; Raupach and Legg 1984), Shuttleworth and Wallace (1985) have recently presented a one-dimensional model for estimating evapotranspiration from sparse crops and soil, which is essentially based on gradient-diffusion models of sensible and latent heat fluxes. They suggested that evapotranspiration models that incorporate simple resistances to vapour flux, such as, stomatal resistance, laminar boundary-layer resistance, and eddy diffusive resistance, and that treat the canopy like a large leaf, are a practical compromise between physical rigour and the demands of field applicability.

In recognition of the possibility that the forest floor evaporation from small plots cleared of salal may have been depressed by the advection of humid air from the surrounding salal canopy onto the treated plots Black et al. (1984; 1985) initiated an investigation of the effects of salal removal from a much larger plot (30 x 40 m) on the

soil water regime, tree transpiration, and tree growth, of a 20-year-old Douglas-fir plantation. The experiment described in this thesis was conducted in conjunction with this larger project, with the intention of partitioning the total stand evapotranspiration between tree transpiration, salal transpiration, and forest soil evaporation.

The objectives of this study were to:

1. design a lysimeter which could be used to measure the evapotranspiration of an undisturbed column of forest soil and salal,
2. measure the evaporation rate of the forest soil after salal removal, and
3. determine the relationship between the aerodynamic transfer resistance to vapour flux and windspeed for a salal canopy.

2. THEORY

The Penman-Monteith combination equation for the latent heat flux from an extensive, isothermal canopy of hypostomatous leaves is (Kelliher 1985)

$$LE = \frac{s(Rn - G) + \rho c_p D_o / r_{Ha}}{s + \gamma r_{va}/r_{Ha} (1 + r_c/r_{va})} \quad (1)$$

where s is the slope of the saturated vapour pressure curve (kPa $^{\circ}C^{-1}$), Rn is the net radiation flux density (W m^{-2}), G is the soil heat flux density (W m^{-2}), ρ is the density of moist air (kg m^{-3}), c_p is the specific heat of moist air (J kg^{-1} $^{\circ}C^{-1}$), γ is the psychrometric constant (kPa $^{\circ}C^{-1}$), D_o is the vapour pressure deficit at the exchange level within the canopy (kPa), r_{Ha} and r_{va} are the average boundary-layer resistances of all canopy leaves acting in parallel for sensible and latent heat transfer respectively (Thom 1972; Shuttleworth 1978; 1979) (s m^{-1}), that is

$$r_{Ha} = r_H/2 \text{ LAI} \quad (2)$$

and

$$r_{va} = r_v/2 \text{ LAI} \quad (3)$$

where r_H and r_v are the boundary-layer resistance to sensible heat and water vapour, respectively, on one side of a leaf, and r_c is the

canopy or surface resistance given by

$$r_c = r_s/LAI + r_v/2\ LAI \qquad (4)$$

where r_s is the stomatal resistance of the side of the leaf with stomata.

Assuming similarity between the boundary-layer resistance to sensible heat and water vapour transfer, i.e., $r_H = r_V$, then (1) can be written as

$$LE = \frac{s(Rn - G) + \rho c_p\ D_o/r_{Ha}}{s + \gamma\ (1 + r_c/r_{Ha})} \qquad (5)$$

To use (5) for estimating the latent heat flux density from a plant canopy requires that the vapour pressure deficit, D_o, be measured within the canopy at a position considered to be the source level for water vapour. If the vapour pressure deficit is measured at a height above the canopy then extra resistances to vapour and sensible heat transport must be added in series with the boundary-layer resistances. These extra resistances are due to the eddy diffusive resistance of the air layer between the transpiring canopy and the meteorological sensors.

Shuttleworth (1978; 1979) and Black et al. (1970) showed that when the Penman-Monteith equation is used to estimate the latent heat flux density from one layer of a multilayered canopy using meteorological measurements made at a height above the canopy of interest then the latent heat flux density originating from below the layer of interest

must be taken into consideration. Using Shuttleworth's (1978; 1979) theory, Kelliher (1985) shows that the latent heat flux density from layer i can be written as

$$LE'_i = \frac{s(Rn_i - G) + \rho c_p (D_i - \delta_i)/r_{Ai}}{s + \gamma (1 + r_{ci}/r_{Ai})} \tag{6}$$

where LE'_i is the difference between LE_i and LE_{i-1}, Rn_i is the net radiation flux density above the layer, D_i is the vapour pressure deficit above the layer,

$$\delta_i = [s(Rn_{i-1} - G)(r_{Hi}/2\ LAI_i)) + (s + \gamma)\ LE_{i-1}\ r_{ai}]/\rho c_p \tag{7}$$

r_{Ai} is the bulk areodynamic resistance to sensible and latent heat transport of layer i and is defined by

$$r_{Ai} = r_{Hi}/(2\ LAI_i) + r_{ai} \tag{8}$$

and r_{ci} is the canopy resistance, which from (4) is

$$r_{ci} = r_{si}/LAI_i + r_{vi}/(2\ LAI_i) \tag{9}$$

If the soil heat flux density below the canopy of interest is equal to Rn_{i-1} and LE_{i-1} is zero or very nearly zero then δ_i is approximately zero and can be ignored. Under these conditions (6) simplifies to

$$LE'_i = \frac{s(Rn_i - G) + \rho c_p\ D_i/r_{Ai}}{s + \gamma (1 + r_{ci}/r_{Ai})} \tag{10}$$

When the canopy is completely wet the canopy resistance becomes zero and (10) simplifies to

$$LE_i' = \frac{s(Rn_i - G) + \rho c_p D_i / r_{Ai}}{s + \gamma} \qquad (11)$$

Equation (11) can be rearranged to calculate the bulk aerodynamic resistance to water vapour transport as follows

$$r_{Ai} = \frac{\rho c_p D_i}{LE_i' (s + \gamma) - s(Rn_i - G)} \qquad (12)$$

Calder et al. (1984) used this technique in studies of rainfall interception losses from upland heather (Calluna vulgaris L.). They demonstrated that r_{Ai} determined from measurements made during rainfall events were not significantly different from estimates obtained by artificially wetting the foliage with plant sprayers.

3. METHODS

3.1 Site Description

3.1.1 Experimental Site Location

The field experiment was conducted in a Douglas-fir stand located in the Dunsmuir Creek watershed, approximately 30 km southwest of Nanaimo, B.C., and 5 km south of Mt. Hooker (40° 02' N, 124° 12' W). The site is located at an elevation of 450 m on a 2-5° slope with a northeasterly aspect.

The B.C. Ministry of Forests' map of the biogeoclimatic units for the Nootka-Nanaimo area indicates that the Dunsmuir Creek watershed lies in the transition zone between the Nanaimo and Georgia Wetter Maritime Coastal Douglas-fir Variant, and the East Vancouver Island Drier Maritime Coastal Western Hemlock Variant (Anon 1979).

3.1.2 Stand Structure

The stand was planted to Douglas-fir in 1963, but substantial natural regeneration has occurred so that the stand density varies considerably and is as high as 5,000 stems per hectare in places. The major conifer species in the stand are Douglas-fir and western hemlock (Tsuga heterophylla (Raf.) Sarg.). There is also a minor component of western red cedar (Thuja plicata Donn), western white pine (Pinus monticola Dougl.), and lodgepole pine (Pinus contorta var. latifolia Dougl.). The estimated average height of the trees was 7-8 m, with the exception of the western white pines which were much taller.

Red alder (Alnus rubra Bong.) and Pacific willow (Salix lasiandra Benth.) were present around depressional areas with restricted drainage, which remained moist even after extended periods of warm dry weather.

The understory vegetation was predominantly salal, with bracken fern present on moister sites, and a small amount of dull Oregon-grape (Mahonia nervosa (Pursh) Nutt.) interspersed with the salal. The dominant moss growing in the surrounding mature forest was step moss (Hylocomium splendens (Hedw.) B.S.G.).

Several large openings in the stand were found to be due to group dying of trees infected by the root rot pathogen Armillaria mellea. Most of the western white pines displayed the symptoms of white pine blister rust (Cronartium ribicola J.C. Fischer ex Rabh.) infection and western gall rust (Endocronartium harknessi J.P. Moore) was observed on several of the larger lodepole pines.

3.1.3 Soil Description

On the basis of a field examination, by Mr. Paul Sanborn (Dept. of Soil Science, Univ. of B.C.), the soil was classified as a Duric Dystric Brunisol (Appendix I).

The fine bulk density (Table 1.1) was determined by removing all the soil from holes of approximately 1 liter in volume extending from the 5 to 30 cm and 35 to 60 cm depths respectively. The exact volume was determined by lining the hole with a plastic bag and filling it with a measured volume of water. The volume of fine soil particles was obtained by subtracting the volume of the coarse fragments (> 2 mm

Table 1.1 Bulk density of the fine (< 2 mm) soil fraction in the the cleared and uncleared plots at the Dunsmuir Creek site

Depth (cm)	Fine Bulk Density (kg m^{-3})
Uncleared Plot	
15-25	770
40-50	950
60-70	890
Cleared Plot	
10-20	880
40-50	860
70-80	1,150

diameter) from the measured hole volume.

Fifteen soil samples were collected at several depths from 2 soil pits and sieved to remove the greater than 2 mm diameter fraction. The hydrometer method was used to determine the percent sand, silt, and clay size particles in each sample. The coarse fragment content in all samples was greater than 20% and therefore the soil was classed as a gravelly sandy loam to loamy sand (Tables 1.2 and 1.3).

The volumetric stone fraction was determined by removing all of the material from a pit measuring 0.5 m x 0.5 m x 0.7 m deep. The volume of the pit was calculated by determining the dry mass of the greater than 2 mm diameter and less than 2 mm diameter fractions; dividing the former by the measured density of the stones (2,520 kg m^{-3}) and dividing the latter by the average fine bulk density (900 kg m^{-3}), and then summing the two quotients. The volumetric stone fraction was found to be approximately fifty-three percent.

The soil water retention characteristics of the soil were determined from desorption measurements made on undisturbed soil cores, obtained with 5.4 cm I.D. x 3 cm long brass cylinders. Soil cores were collected from two soil pits. Two cores were taken from each of the 10 and 40 cm depths and one was taken from the 60 cm depth. All desorption measurements were made using a pressure membrane apparatus (Soil Moisture Equipment Corp., Santa Barbara, Calif., USA). After each equilibration, the sample was weighed and then resaturated for 24 hours before applying the next pressure step. Samples from a single depth were averaged to give 3 retention curves.

Table 1.2 Soil texture analysis (%) for cleared and uncleared plots at the Dunsmuir Creek site. The samples were taken from the soil excavated for the bulk density measurements listed in Table 1.1

Depth (cm)	Sand	Silt	Clay	Texture
Uncleared Plot				
10	66.2	29.6	4.2	SL
40	75.6	21.7	2.7	LS
Cleared Plot				
10	69.9	26.0	4.1	SL
40	72.8	23.9	3.3	SL/LS
60	73.4	25.4	1.2	LS

Table 1.3 Soil texture analysis (%) of cores used to obtain water retention curves for cleared and uncleared plots at the Dunsmuir Creek site. The values are averages for two cores, except for the 60 cm depth value which was for one core. The cores were taken 1.5 m from the samples in Table 1.2

Depth (cm)	Sand	Silt	Clay	Texture
Uncleared Plot				
15	53.4	40.0	6.6	SL
40	66.0	29.5	4.5	SL
60	70.2	26.6	3.2	SL
Cleared Plot				
10	71.8	25.0	3.2	SL
40	76.0	21.4	2.6	LS
70	64.0	32.6	3.4	SL

The volumetric water content for each sample was corrected by subtracting the volume of the coarse fragments (> 2 mm diameter) from the volume of the soil core. The bulk density of the fine fraction in these samples ranged from 810 to 990 kg m^{-3} (Table 1.3).

The soil water retention curves are shown in Figures 1.1 and 1.2. Figure 1.1 shows the entire 0 to -1.5 MPa curves, while Figure 1.2 shows the wet end curves for the range 0 to -0.1 MPa. These curves are typical of a coarse textured soil.

3.1.4 Experimental Plot Layout and Salal Removal

In 1983 a meteorological tower was erected in approximately the center of the stand. Wind direction data, gathered in 1983, showed that the prevailing daytime winds were from the east on fine days. Changes in wind direction generally moved through the south with westerlies accompanying storm fronts. Two areas within the stand, similar in topography and stand density, were selected for plot loctions. Plots measuring 30 x 40 metres were then marked out in these areas, with the 40 metre dimension oriented along the east-west axis. The plot to be cleared of salal was located to the northwest of the meteorological tower so that air passing over it would not be picked up by sensors on the tower. The untreated plot was located to the east of the tower so that water balance measurements made on the untreated plot could be related to energy balance measurements made over the stand.

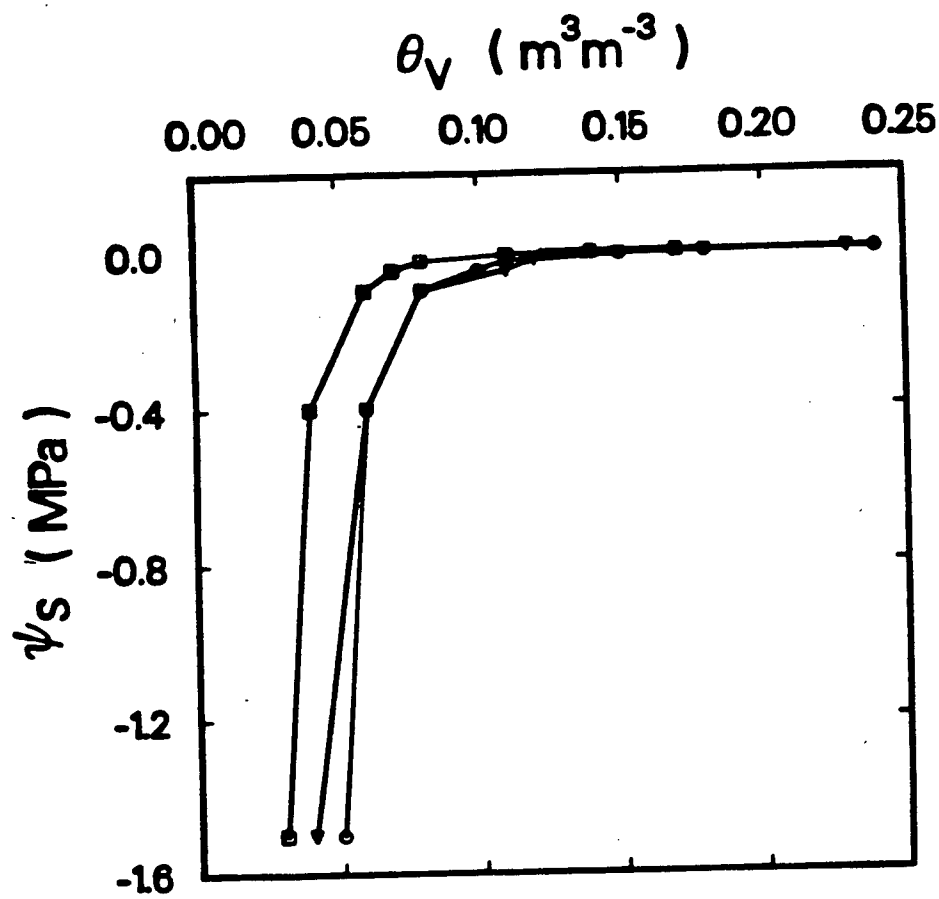

Figure 1.1 Soil water retention (desorption)curves for the soil at the Dunsmuir Creek site (1 MPa = 10 bars) ▽ 10 cm, 0 40 cm, □ 60 cm.

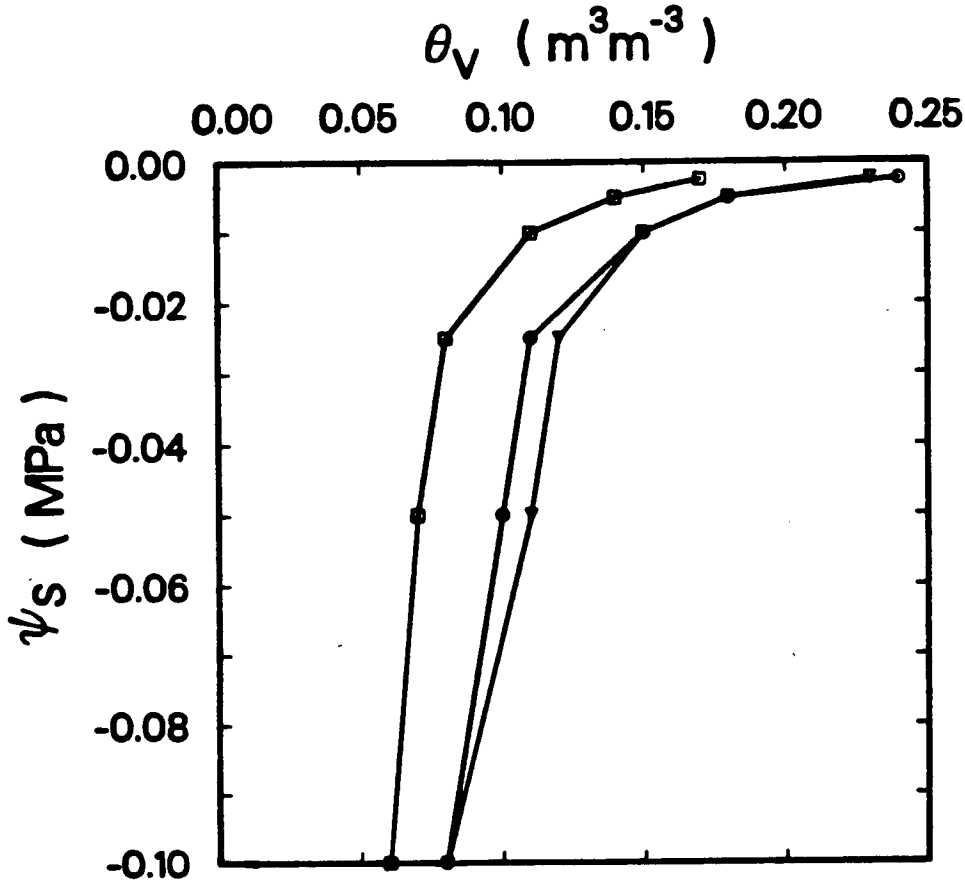

Figure 1.2 Wet end soil water retention (desorption) curves for the soil at the Dunsmuir Creek site (1 MPa = 10 bars) ▽ 10 cm, ○ 40 cm, □ 60 cm.

In April 1984 one metre quadrat samples of the understory foliage were collected from ten locations within the plot to be cleared and from six locations around the outside edge of the untreated plot. Immediately following the foliage sampling all of the understory vegetation within the treatment plot was manually destroyed with sandvik clearing axes and clippers. New foliage was observed to be sprouting from salal stolons by the middle of July. At the end of the growing season, October 1984, four, one metre quadrat samples of foliage were collected from the treated plot to obtain an estimate of the regrowth in leaf area. In the untreated plots, two, one metre quadrat measurements of foliage were made to estimate the increase in leaf area during the growing season. In April 1985, the herbicide Garlon 4a (Dow Chemicals), was applied to the regrowth in the cleared plot. No significant regrowth during 1985 was observed after this application.

3.2 Measurements

3.2.1 Salal Leaf Area Index

The leaf area index (LAI) for all the understory vegetation collected in the one metre quadrats was measured using the Licor Model LI 3000 portable leaf area meter, with the 3050A conveyor attachment (Li-Cor Inc., Lincoln, NE, U.S.A.). The meter was calibrated between samples using an aluminum disk of known area.

Each quadrat sample was divided into two subsamples. All the leaves from the smaller subsample were stripped off the twigs and passed

through the meter. All the leaves and twigs from the smaller subsample and the larger subsample were then placed in three separate paper bags and oven dried, at 70°C, to a constant mass. The final dry mass of each portion of the sample was measured and the leaf area of the sample was estimated using

$$LA = LA1\ (ML + MT + M2)/(ML + MT) \qquad (13)$$

where LA is the total leaf area of the sample, LA1 is the measured leaf area of the smaller subsample, ML and MT are the dry masses of the separated leaves and twigs from the smaller subsample, and M2 is the dry mass of the larger subsample.

Since the foliage samples were collected from one square metre quadrats, the calculated leaf area was a direct estimate of the LAI, on a projected leaf area basis, of the understory vegetation. The accuracy of the subsampling procedure was checked by measuring the leaf area of the entire first sample and comparing the measured leaf area with that estimated from Equation (13). The estimated leaf area was found to agree with the measured leaf area to within five percent. The understory LAI, within the stand, ranged from 0.5 to 3, and the average for the plot area was 1.7.

3.2.2 Root Zone Soil Water Content and Potential

In April 1984, five thin walled aluminum neutron moisture probe access tubes (48 mm inside diameter) were installed in the soil within each plot. The technique described by Kelliher (1985) for producing

holes in the soil, into which the aluminum access tubes can be placed, was found to be impractical due to the extreme stoniness of the soil.

To install a tube a trench 1 m long by 30 cm wide was dug down to the compact till. The soil was separated according to depth interval and covered to prevent evaporation. A vertical notch the same diameter as the tube was made at one end of the trench and the tube was pushed firmly into the notch. The depth of soil to the compact till was measured, and at each 5 cm depth interval 2 soil samples were collected in aluminum soil sampling cans for neutron hydroprobe calibration purposes. The trench was then back filled and compacted layer by layer to achieve as close to the original density as possible. The surface organic layer, which had initially been carefully scalped off, was replaced. The neutron probe of a Campbell Pacific Nuclear hydroprobe (model CPN 503, Sacker Scientific Company, Edmonton, Alta.) was lowered into the aluminum access tube and a 30 second reading was taken at each 15 cm depth interval, beginning at 15 cm and continuing to the bottom of the tube. The soil samples were weighed, dried at 105°C to a constant mass, and the volumetric soil water content was calculated using the following equation

$$\theta_v = W_c \, \rho_{fs} \, (1 - f)/\rho_w \qquad (14)$$

where W_c is the water content of the fine fraction of the gravimetric samples on a dry mass basis, ρ_{fs} is the bulk density of the fine fraction, and ρ_w is the density of liquid water.

Twenty more tubes were installed, following the same procedure, into a contiguous clearcut area. Gravimetric soil samples from all the trenches were used in calibrating the neutron hydroprobe. As the soil dried, soil pits were dug near selected calibration tubes and gravimetric samples were collected from the 45 cm depth. These samples were treated as described above to obtain calibration data for dry soil. The 45 cm depth was used to ensure that the surface could not influence the hydroprobe measurements, even at very low soil water contents.

The calibration of the neutron hydroprobe covered a range of volumetric water contents from 0.04 to 0.36 $m^3\ m^{-3}$ (Appendix 2). The linear equation found to fit the data was

$$\theta_v = 0.217\ (c/c_s) - 0.075 \qquad (15)$$

where θ_v is the volumetric water content of the whole soil, c is the neutron count for a 30 second time interval with the probe in the soil, and c_s is the neutron count for a 30 second time interval with the probe in the shield.

Independent calibration of the same hydroprobe by Kelliher (1985) and Giles (1983) for soils in Courtenay, B.C., and Mesachie Lake, B.C., respectively, yielded the following equations

$$\theta_v = 0.224\ (c/c_s) - 0.009 \qquad (16)$$

$$\theta_v = 0.23\ (c/c_s) - 0.021 \qquad (17)$$

Equation (15) was based on almost twice the sample sizes of (16) and (17), and the site was considerably stonier, however, all three equations are very similar.

On August 2, 1984, thermocouple psychrometers (model PCT-55, Wescor Inc., Logan, Utah, U.S.A.) were installed, in pairs, at 15, 45, and 75 cm depths, in the cleared and uncleared plots. The psychrometers were placed in 15 cm long holes, made with a screwdriver, in opposite faces of a carefully excavated soil pit. Loose soil was tamped into the holes to insure good contact between the ceramic cups and the surrounding soil. The thermocouple lead wires were wrapped around the pit and then lead to the surface. The soil pit was then refilled and tamped to a density approaching its original condition. The thermocouples were cooled and measured using a Wescor model HR-33T dew point microvoltmeter on both psychrometric and dewpoint modes.

3.2.3 Meteorological Measurements

A basic automated meteorological station was maintained, in a more recently planted area 300 metres from the research plots, during the growing seasons from 1983 to 1985. The climate variables recorded on an hourly basis were solar irradiance, air temperature, atmospheric humidity, soil temperatures at 0, 20 and 50 cm, and windspeed (1 m height). Wind direction was measured in 1983, 1984 and during the latter half of the 1985 field season. The data were logged on a Campbell Scientific CR21 Micrologger and recorded on cassette tape.

At the research plots, meteorological measurements were made above the tree canopy in 1984 and 1985. In 1984 meteorological measurements

were also made below the tree canopy within the cleared plot, and in 1985 meteorologial measurements were made below the tree canopy in the uncleared plot.

The net radiation flux density above the stand was measured using a Swissteco (S-1) net radiometer. In 1984, net radiation flux density below the tree canopy in the cleared plot, was measured with a Swissteco (S-1) net radiometer. In 1985, the net radiation flux density below the tree canopy in the uncleared plot was measured in two locations. At the first, 2 m to the south of the weighing lysimeter a Swissteco (S-1) was used, while at the second, 30 cm directly above the lysimeter containing salal, a Swissteco miniature (ME - 1)net radiometer was used.

The soil heat flux density was measured using a pair of soil heat flux plates (Middleton and Co. Pty, Ltd., South Melbourne, Australia) positioned 5 cm below the soil surface. A pair of integrating thermometers with 5 temperature diodes spaced at 1 cm intervals was placed in the soil, near the heat flux plates, to measure the change in the mean soil temperature for the 0-5 cm depth. Gravimetric soil samples from the 0-5 cm layer were periodically collected and the volumetric water content was determined, as this has a strong influence on the volumetric heat capacity of the soil. The bulk density of the organic layer was found to be 0.18 kg m^{-3}. The rate of change of the energy stored (W m^{-2}) in the 0-5 cm layer was calculated using

$$M = C(\Delta T/\Delta t)\ Z \qquad (18)$$

where C is the volumetric heat capacity of the soil sample, ΔT is the change in temperature, Δt is the time interval (usually 30 min.), and Z

is the depth of the soil heat flux plates. The soil heat flux (W m^{-2}) at the surface was computed from

$$G_0 = G_5 + M \qquad (19)$$

where G_5 is the soil heat flux density measured at 5 cm with the soil heat flux plates.

The windspeed was measured above and below the stand with sensitive Casella (C.F. Casella and Company, Ltd., London, England) cup anemometers. The anemometer below the stand was positioned approximately 30 cm above the salal canopy adjacent to the lysimeter. A hotwire anemometer (Wilh, Lambrecht KG, Göttingen, West Germany) was used occasionally to measure low windspeeds above the salal canopy.

Air temperature and humidity, below the tree canopy in the uncleared plot, was measured with an FD300 silicon diode psychrometer, ventilated at 3-4 m s^{-1}, and positioned approximately 30 cm above the salal canopy. The silicon diode psychrometer was repeatedly calibrated, during the course of the experiment, with an Assmann psychrometer.

All meteorological data were electronically recorded using a Campbell Scientific model CR-7 data logger, printed out by a Campbell Scientific CR56 printer, and recorded on cassette tapes. A continuous record of the below tree canopy net radiation flux density, measured by the miniature net radiometer above the lysimeter, was obtained with a Soltec (Model VP-6723S) chart recorder.

3.2.4 Forest Soil Evaporation

Daily total evaporation from an undisturbed column of forest soil was measured in August 1984 using a weighing lysimeter (described in

Section 3.3). A location near the centre of the cleared plot was selected for the lysimeter, in order to minimize advection from the surrounding salal canopy. A steel lined well (1 m x 0.65 m I.D. x 0.003 m wall thickness) with a sloping concrete floor and drainage hole, was prepared in advance of the soil core being excavated. In order to avoid damaging the area surrounding the lysimeter location a skyline of 1.58 cm diameter wire rope was installed over the work area and all soil was carefully loaded into a container suspended from the skyline and removed. The skyline was also used to bring the soil core to the lysimeter wall.

The soil core was obtained by positioning a stainless steel cylinder, 0.6 meters inside diameter by 0.75 meters deep and 0.48 cm wall thickness, over a portion of the forest floor. A 0.48 cm thick stainless steel plate with a slightly larger diameter than the cylinder was placed on top of the cylinder. Twenty 25 kg steel discs were then stacked on the cylinder to provide a downward force. A trench was then dug around the bottom edge of the cylinder and as soil was removed the cylinder slowly slid down, isolating an undisturbed core. When the cylinder was down the full 0.75 m the weights were removed and cribbing was carefully placed on the top edge of the cylinder and the weights replaced. This allowed the cylinder to be forced down another 2.5 cm so that the cylinder was below the surface level. Webbed ducting tape was wrapped around the top edge of the cylinder to hold the organic layer in place. Positioning the top edge of the cylinder below the surface minimized the radiation load on the lysimeter walls and the heat conduction through the walls to the soil inside.

When the cylinder had been forced down to its final depth the weights and cribbing were removed and the stainless steel plate, that had supported the weights, was used to sever the bottom of the soil core. This was accomplished by a combination of excavating under the soil core and forcing the stainless steel plate under with hydraulic jacks.

Wire rope (0.48 cm diameter) was positioned under the stainless steel plate at the bottom of the isolated soil core and the sample was hoisted into the air, suspended on the skyline. The sample was lowered onto a tray which was slightly larger diameter than the cylinder. The tray had short walls 8 cm in height, and 5 cm wide stainless steel straps which were welded to the bottom of the tray and ran up the side of the cylinder walls and protruded 10 cm above the soil surface (Figure 1.3). The isolated soil core was then suspended from these three metal straps. The gap between the cylinder and the support tray walls was sealed with ducting tape. The support tray was watertight.

The lysimeter sample was moved to the lysimeter well on the skyline and lowered into position. The sample was suspended from the lysimeter beam by three 0.48 cm diameter wire ropes. Each of the suspension wires had a 15 cm turnbuckle spliced into it so that the soil core could be levelled in the well. This was important because it facilitated keeping the width of the annulus uniform. The annular area was 17% of the lysimeter area.

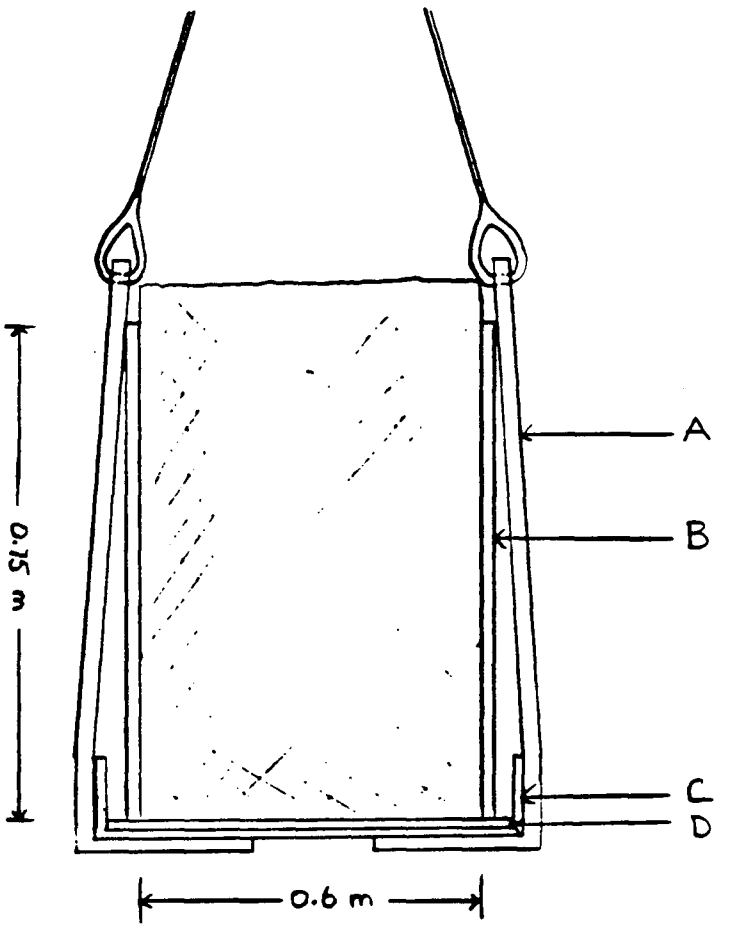

Figure 1.3 Cross-section through the lysimeter cylinder and the suspension tray; A = stainless steel straps, B = stainless steel cylinder, C = stainless steel pan with short side walls, D = stainless steel plate used to sever the bottom of the isolated soil column.

3.2.5 Understory Evapotranspiration

The understory evapotranspiration rate was measured during June and July 1985, using a second lysimeter constructed the previous summer in the uncleared plot. The method of lysimeter construction and installation was similar to that described for the lysimeter in the cleared plot. A few modifications were made to improve the lysimeters performance (described in Section 3.3), and in the technique for obtaining the soil plus salal community sample.

The stainless steel cylinder was positioned over a salal community which was a bit clumped. A clump was chosen in order to minimize damage to the roots of plants which might be growing close to the cylinder walls. Cribbing was built up on top of the cylinder and 455 kg of steel weights were loaded onto the cribbing. After isolating the salal and soil core the sample was well watered and allowed to drain for one day. The sample was moved into the lysimeter well, suspended from the lysimeter beam, and left over the winter. The total mass of the soil, lysimeter cylinder and suspension tray, with the soil column fully recharged with moisture was approximately 400 kg.

In the spring of 1985, stomatal resistance measurements were conducted on salal plants growing within the lysimeter and on plants surrounding the lysimeter. The measurements were made with a Ll-Cor, Model LI-1600 steady state porometer.

Understory evapotranspiration was measured continuously from June 21 to July 11. The change in lysimeter mass was recorded by the CR7 data logger and a continuous trace was obtained with the Soltec chart

recorder. The stomatal resistance of salal plants growing in and around the lysimeter was measured periodically.

On July 8 all of the salal in the lysimeter was clipped and the bare soil evaporation rate was measured for 3 days.

3.3 Weighing Lysimeter System

3.3.1 Design and Construction

In order to minimize the amount of excavation necessary to install the lysimeter and its weighing mechanism an above ground balance type lysimeter was constructed (Figure 1.4). A 15 cm x 15 cm steel I-beam was used as the suspension beam. A 15 cm O.D., thick walled, steel support post, was used to elevate the suspension beam above the salal canopy. The support post was positioned in a hole dug down to the compact till and then back filled with concrete to ensure that it was rigid.

Tubular extensions, approximately 0.40 m long, were welded onto both ends of the suspension beam, in order to reduce shading by the beam of the lysimeter. The extensions were constructed of 4.5 cm O.D. pipe with a 3.2 mm wall thickness. The extensions were braced by triangulated steel strapping (3.8 cm wide x 0.64 cm thick), welded to both sides of the extension tubes and the top plate of the I-beam (see Figure 1.4). This proved to be a rigid arrangement and it achieved a substantial reduction in the portion of the lysimeter's sky view which was occupied by the suspension beam. To further reduce the shading effect of the

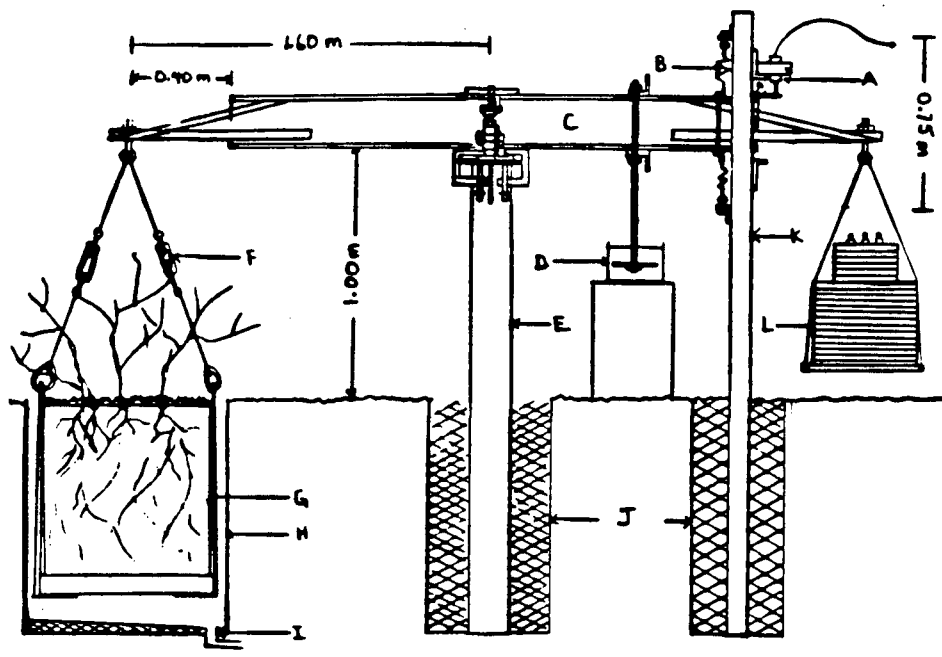

Figure 1.4 Side view of the lysimeter and weighing mechanism, showing the location of the main components; A = LVDT, B = top spring, C = suspension I beam, D = dash pot, E = support post, F = turnbuckle, G = lysimeter cylinder, H = steel retaining wall, I = sloping concrete floor and drain, J = concrete, K = 7.6 cm steel channel guides, L = steel plates.

weighing mechanism, all of the above ground components were positioned north of the lysimeter well.

The lysimeter sample and the counterweights were suspended from the support beam by 3 wire ropes which were fastened to eye-bolts that were located near the ends of the extensions. The ring of the eye-bolt was welded so that it could not open up under heavy loading. All the wire ropes were run through wire rope thimbles wherever they had to take a sharp bend, and the ends were secured with 2 wire rope clamps to prevent slipping.

The suspension beam pivoted on 2 knife edges which were constructed of high speed tool steel blanks embedded in right angle grooves at 45° to the horizontal, machined in 2.54 cm thick blocks of soft steel (Figure 1.5). The knife edges bore on another set of high speed tool steel blanks which were also embedded in soft steel. The bearing blanks were set in slots which were slightly deeper than the blank, thereby creating a small lip which prevented the knife edges from sliding off the polished surfaces. The combination of the high speed tool steel embedded in the soft steel blocks will be referred to as top and bottom pivot blocks, for the knife edge and bearing surface components respectively, throughout the rest of the text.

The top pivot blocks were bolted onto a steel web which had been welded at a right angle to the suspension beam, at it's midpoint (Figure 1.6). The top pivot blocks were bolted with a single 1.90 cm bolt positioned at the centre of the block so that when the suspension beam was lowered down onto the knife edges the pivot blocks could rotate,

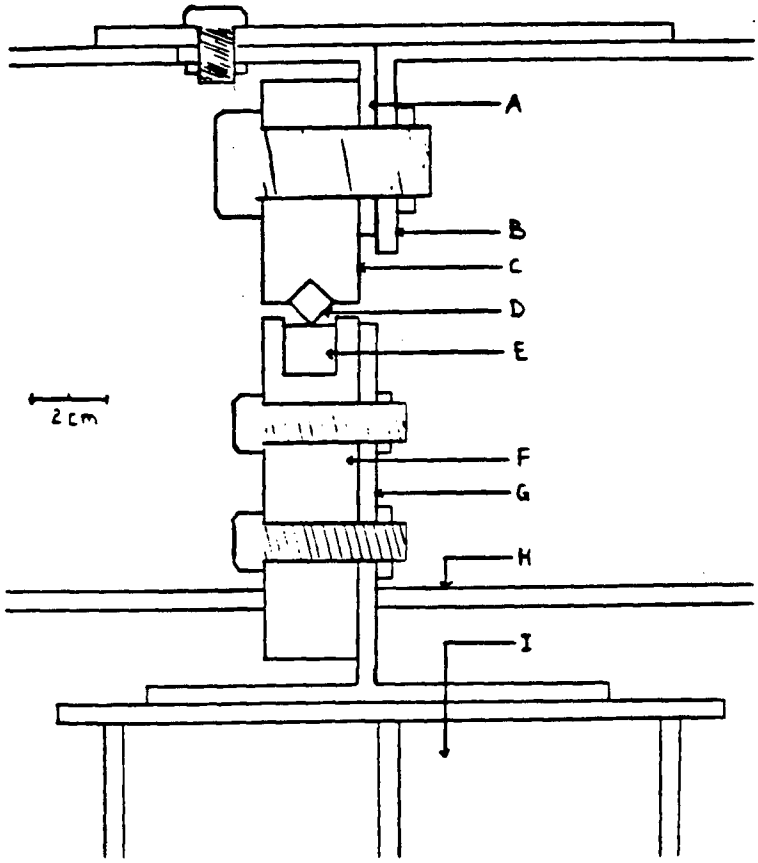

Figure 1.5 Side view of the fulcrum assembly; A = 5 cm steel angle iron, B = steel web welded perpendicular to the suspension beam, C = 2.54 cm thick soft steel top pivot block, D = hard tool steel bit, 5 cm long, E = hard tool steel bit, 5 cm long, F = 2.54 cm thick soft steel bottom pivot block, G = web of a short segment of I-beam, H = bottom plate of the suspension I beam, I = support post.

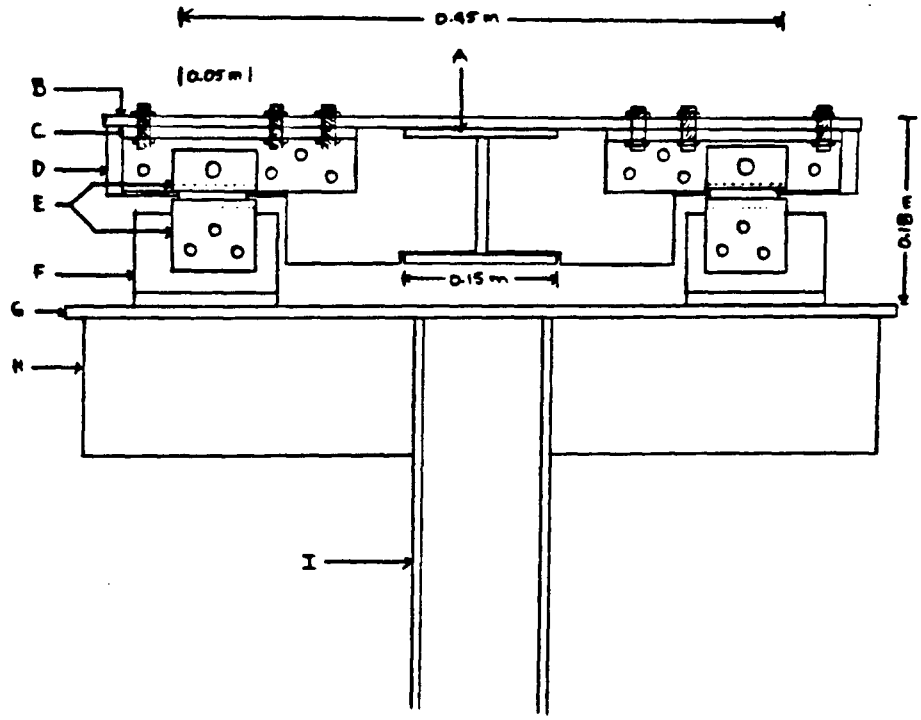

Figure 1.6 End view of the fulcrum assembly; A = suspension I beam, B = top plate of the web welded across the suspension beam, C = 5 cm angle iron, D = steel web, E = top and bottom pivot blocks containing the knife edge and bearing surface in machined slots, F = short segment of I-beam with one plate removed, G = support platform, H = strengthening web, I = support post.

and the weight would be evenly distributed across the 5 cm length of each knife edge. The knife edges were separated by 0.35 m in order to provide lateral stability to the support beam, and were positioned at the midline of the I-beam. This arrangement was found to be superior to an earlier arrangement where ball bearing pivots were positioned below the bottom plate of the suspension beam.

The bottom pivot blocks, containing the hard bearing surfaces, were bolted to the web of short lengths of 15 x 15 cm I-beam, from which one plate had been removed to form a T. The flat surface of each T rested on a steel support platform which was welded to the top of the steel support post. A web was welded under the steel support platform to give it added strength. The top and bottom pivot blocks could be moved around, to a limited extent, on the support platform. This facilitated adjustment of the lysimeter container within the well. Once the lysimeter was positioned so that it could not come in contact with the well walls the bottom pivot blocks were firmly fixed in place on the support platform with large metal C type clamps.

A simple dash pot filled with heavy weight oil for damping out vibration due to gusts of wind was fastened onto the suspension beam approximately 0.80 m from the fulcrum, on the counterweight end (see Figure 1.4). The counterweights were 25 kg and 10 kg circular metal plates. For fine adjustments numerous smaller metal plates of known mass were available. Standard weights were used for calibration purposes.

A matched pair of stainless steel springs (1.27 cm I.D. x 16.83 cm long, 1.59 mm wire thickness, 107 coils) was attached to the top and

bottom of the suspension beam at a point 0.98 m from the fulcrum (Figure 1.7). With the suspension beam held in a level position each spring was tensioned equally. Gifford et al. (1982) used matched pairs of springs to damp wind induced oscillations, and they stated that matched pairs of springs reduced the temperature sensitivity of the spring balance apparatus (Appendix III).

Vertical changes in the position of the suspension beam, due to changes in the mass of the lysimeter sample, were detected using DC linear voltage differential transformers (DC-DC LVDT Model D2/100A, RDP Electronics Ltd., Wolverhampton, U.K.). The LVDT was held in a clamping arrangement fabricated from 2.54 cm thick soft steel in order to embed it in a large thermal mass which would not fluctuate rapidly in temperature (Figure 1.8). A micrometer was also fastened to the clamping arrangement so that the voltage at a known and repeatable displacement could be monitored at different temperatures. This technique was useful in demonstrating the stability of the LVDT output voltage.

The voltage supply for the LVDT was provided by a 12 V automotive battery. A voltage regulator (LM317, 180 mA) provided a stable 6 V supply to the LVDT (50 mA). The output voltage was logged by the CR7 every 2 seconds. The maximum, minimum, and mean voltage for each sampling interval was recorded on cassette tape. The output voltage was also continuously recorded with the Soltec chart recorder.

Angle iron cross pieces, which restricted the range of vertical movement of the suspension beam, were bolted on the outer spring

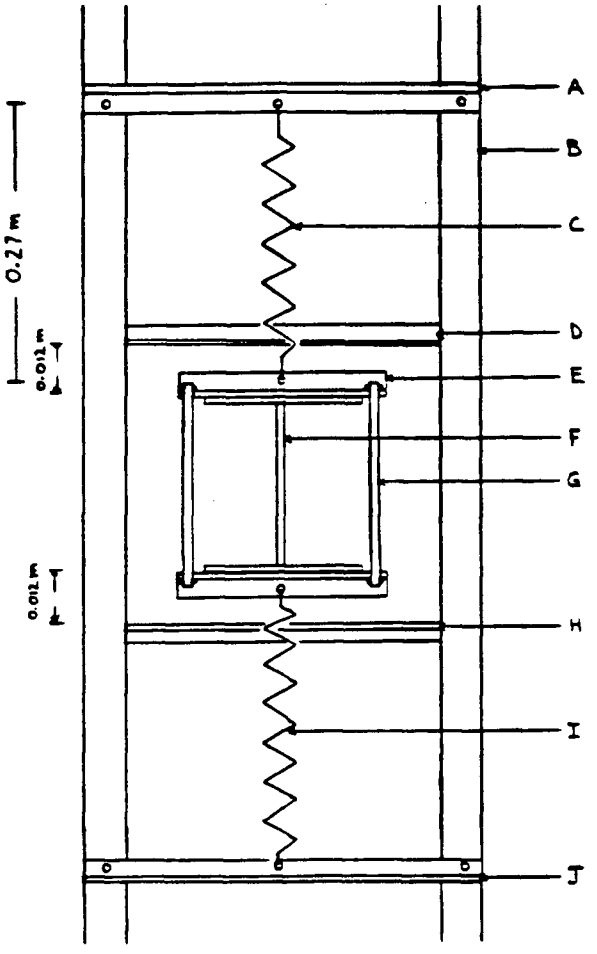

Figure 1.7 End view of the spring attachment; A = 3.8 cm angle iron, B = 7.6 cm steel channel guide; C = stainless steel top spring, D = 3.8 cm angle iron positioned to restrict vertical movement in the suspension beam, E = 3.8 cm angle iron, F = suspension beam, G = 1.27 cm threaded rod, H = 3.8 cm angle iron, I = stainless steel bottom spring, J = 3.8 cm angle iron.

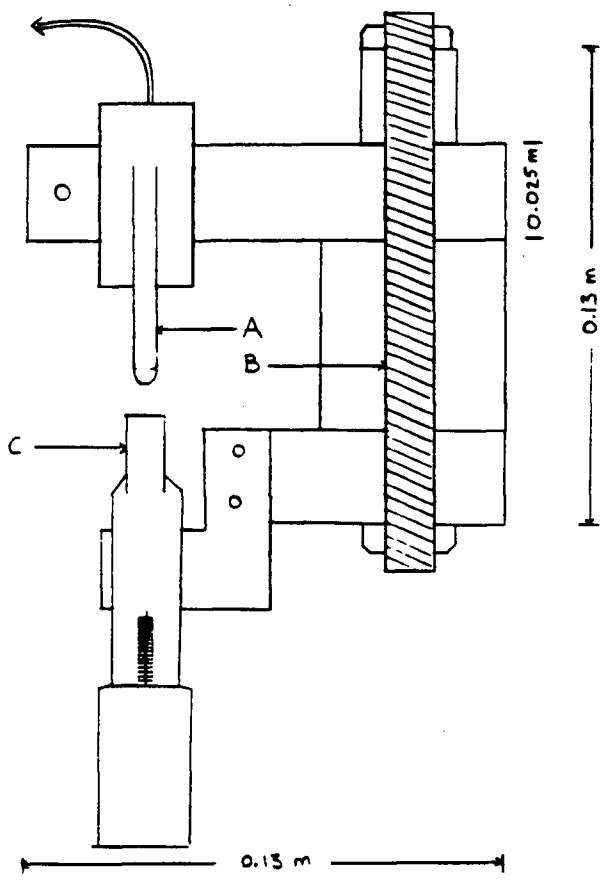

Figure 1.8 Side view of the LVDT mounting arrangement and the position of the calibration micrometer; A = LVDT probe, B = 1.27 cm threaded rod, C = micrometer plunger.

supports. These cross pieces acted as protection for the LVDT by preventing the probe from being pushed beyond its designed range (Fig. 1.7).

The lysimeter was operated as close to neutral as possible; i.e., the beam was maintained near level. This was achieved by removing standard weights from the counterweights as the lysimeter lost mass.

3.3.2 Lysimeter Calibration

Calibration of the lysimeter was accomplished by adding a series of 5, 10, 20, and 50 gram standard weights to the surface of the lysimeter after it had been sealed with 0.1 mm plastic. The LVDT output was continuously recorded on a chart recorder and recorded for one minute sampling intervals on the CR7 data logger. All the weights were then sequentially removed in reverse order as a check on hysteresis. During the course of the experiment, 5, 10, and 20 gram weights were frequently added and removed from the lysimeter and the change in voltage recorded. This provided a check on possible changes in the lysimeter calibration factor.

The calibration data presented in Figure 1.9 are presented in terms of the change in voltage ouput (mV) for a change in lysimeter mass (grams). The sensitivity of the lysimeter apparatus which is given by the slope of the calibration curve was found to be 7.6 mV g^{-1}. The standard error of estimate was 13.57 mV which placed a lower limit on resolution at 1.7 grams. The surface area of the lysimeter was 0.28 m^2 and therefore the loss of 1.7 grams was equivalent to the loss of 0.006 mm of water. A resolution of approximately 2 grams was

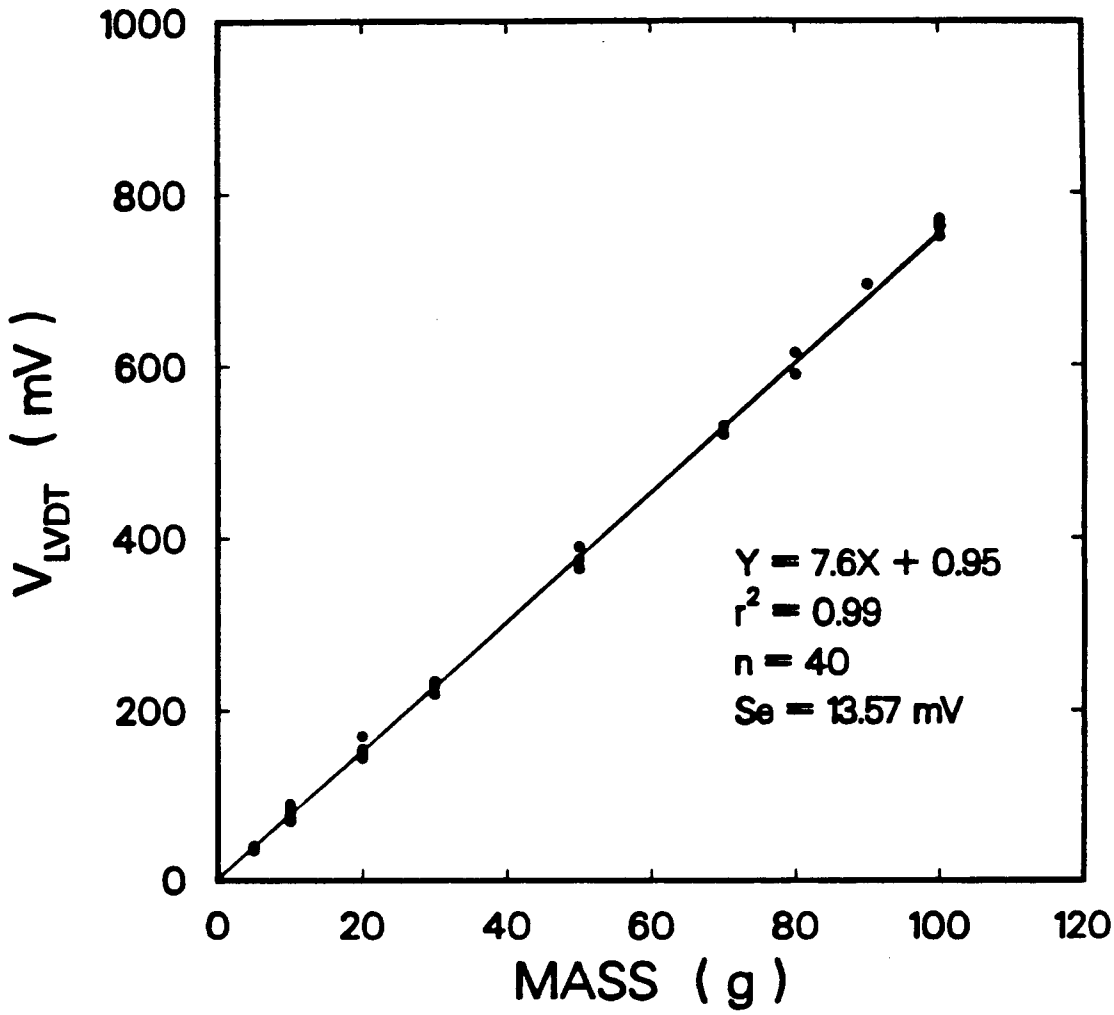

Figure 1.9 Calibration data and equation relating the LVDT output to changes in the mass of the lysimeter.

observed in the field by repeatedly adding 1 and 2 gram weights to the lysimeter.

To test the temperature sensitivity of the LVDT electronics the sensor was repeatedly cooled to 4°C and then allowed to warm to 24°C, the voltage change over this range in temperature was 4 mV or 0.2 mV/°C which was equivalent to 0.0001 mm/°C.

Apparent increases in lysimeter weight during the morning were initially thought to be due to condensation forming on the bottom of the lysimeter. The lysimeter was pulled from the well at a time when the apparent weight gain was greatest and checked for condensation, however no condensation was observed to be present. The apparent weight gains were ultimately attributed to differential heating of the suspension beam which resulted from the irregular pattern of direct solar irradiance below the tree canopy. Painting the beam white reduced the apparent weight gain but was not totally effective. A shade was erected over the weighing mechanism and this resulted in a significant improvement.

At the end of the experimental period the lysimeter was sealed with black polyethylene and the zero drift was monitored for 7 days. Figure 1.10 shows the average apparent change in lysimeter mass due to differential heating of the beam. The shade was not completely effective at 1600 PST when the sun was at a low angle and managed to shine on the counterweight end of the beam. Hourly measurements of evapotranspiration were corrected for apparent weight gains and losses due to differential heating of the suspension beam.

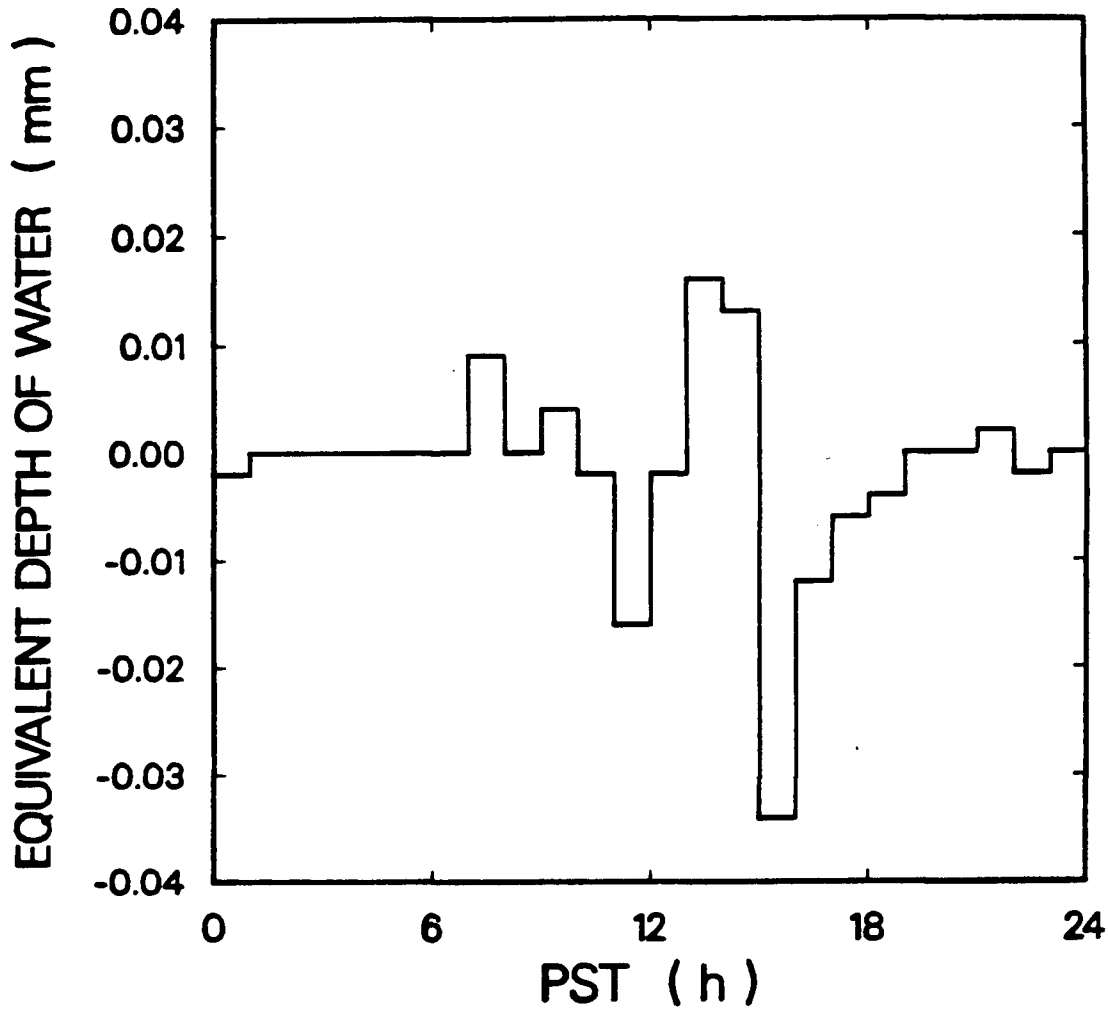

Figure 1.10 Average apparent change in lysimeter mass due to differential heating and expansion of the suspension beam.

On a daily basis the lysimeter zero was very stable. Figure 1.11 shows the apparent change in lysimeter weight after completely shading the entire apparatus.

The following calculation shows that maintaining a uniform radiative heat load on the suspension beam is important to the measurement of hourly evapotranspiration. If the lysimeter end of the suspension beam increases in temperature 1°C and the thermal coefficient of linear expansion of steel is 12×10^{-6} °C^{-1}, then the apparent increase in the mass of the lysimeter would be approximately 5 g, (1°C x 12×10^{-6} °C^{-1} x 400 kg), simply due to the expansion of the beam on one side of the fulcrum.

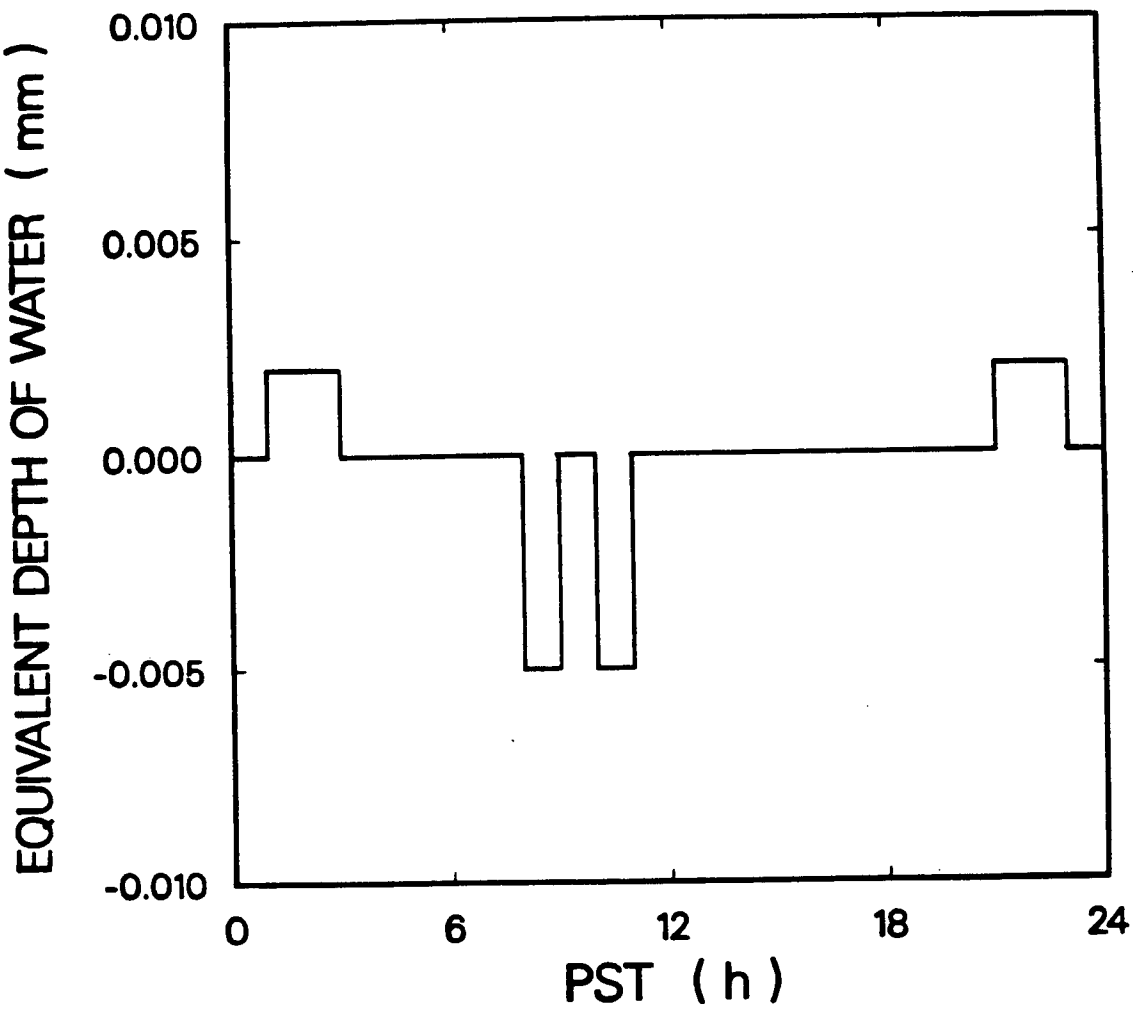

Figure 1.11 Apparent change in lysimeter mass after completely shading the entire weighing mechanism.

4. RESULTS AND DISCUSSION

4.1 Measured Forest Floor Evaporation Rates

The diurnal variability of available energy flux density (i.e. Rn - G) below the tree canopy (A_b) for the days, August 8-15, 1984, during which forest soil evaporation (E_s) was measured with the lysimeter, is shown in Figure 1.12. The interaction between the tree canopy and the temporal variability of the above forest solar irradiance (S_t) in determining A_b is particularly evident for August 8 and 10 (Figures 1.13 and 1.14). While the total S_t for these 2 days was approximately equal, 24.55 and 24.33 MJ m^{-2} d^{-1} respectively, the 24 hr total A_b was 1.91 MJ m^{-2} d^{-1} on August 8 and 1.30 MJ m^{-2} d^{-1} on August 10. The explanation for this is that, on August 10, S_t was low during periods when direct solar radiation could penetrate through gaps in the tree canopy above the lysimeter, and high during periods when the tree canopy effectively intercepted the bulk of the solar radiation.

Over the eight day period, the daily total S_t ranged between 9.52 and 24.55 MJ m^{-2} d^{-1}, and the daily average vapour pressure deficit above the canopy ranged between 0.40 and 0.90 kPa (Figure 1.15). The tipping bucket rain gauge, located at the meteorological station, recorded 3.7 mm of precipitation on August 5 and 6, and from 0200 - 0300 PST on August 13, 0.9 mm of precipitation was recorded.

The 24 hr total E_s was found to range between 0.08 and 0.34 mm d^{-1} (Figure 1.16). The daily evaporation rates were large during the

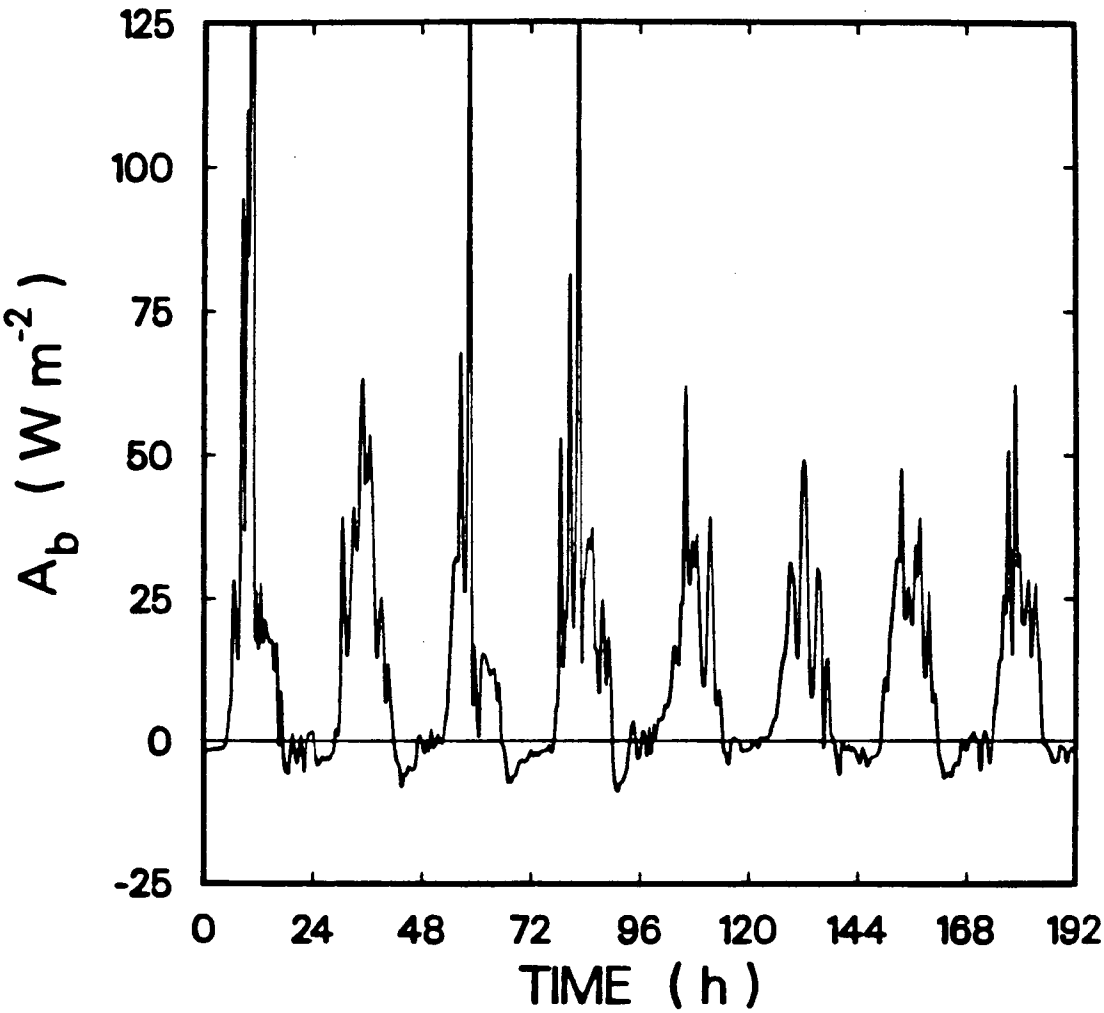

Figure 1.12 Diurnal variability of the below canopy available energy flux density (A_b) for the period August 8-15, 1984.

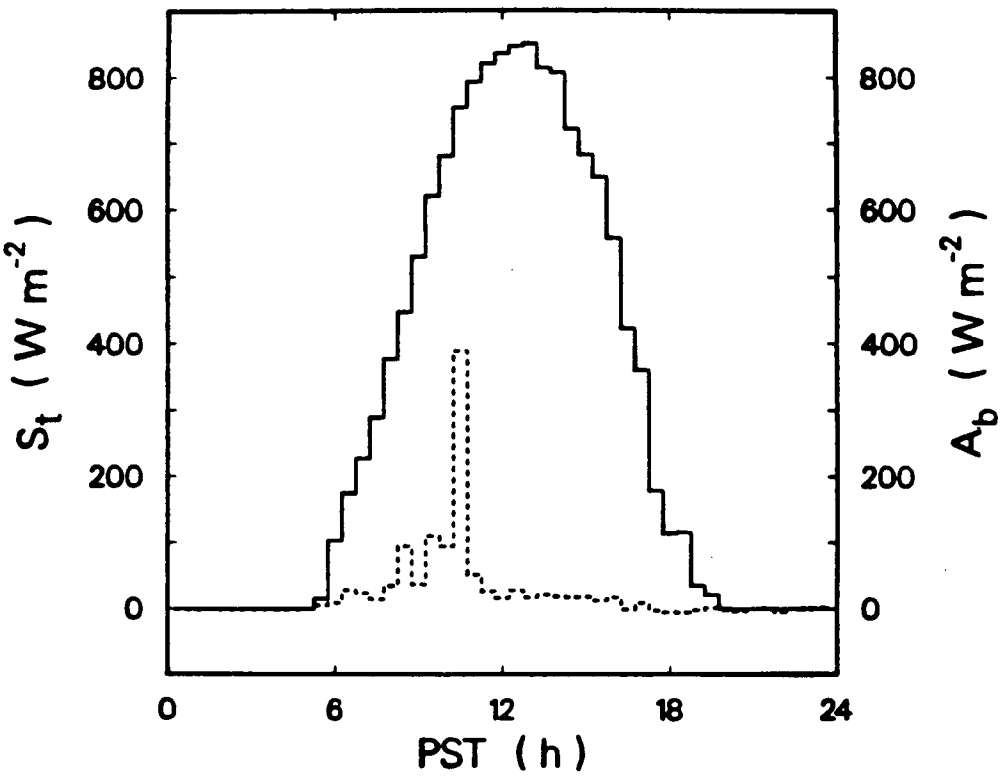

Figure 1.13 Solar irradiance measured above the tree canopy (S_t(——)) and the available energy flux density below the tree canopy (A_b (-----)) for August 8, 1984.

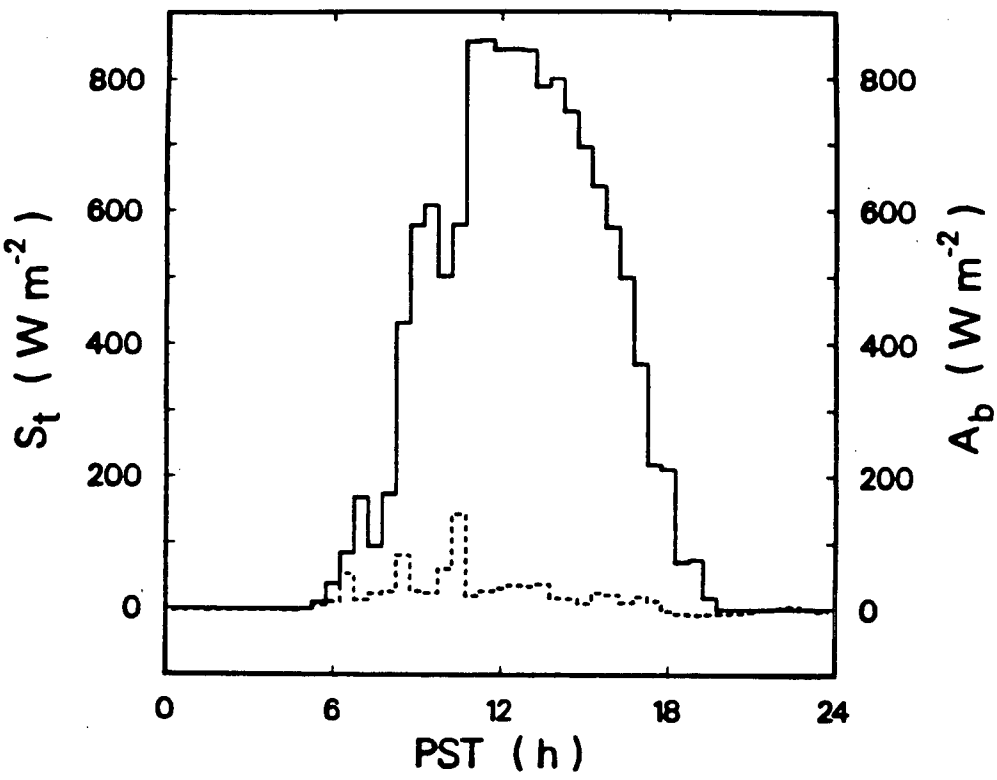

Figure 1.14 Same as for Figure 1.13 except for August 10, 1984.

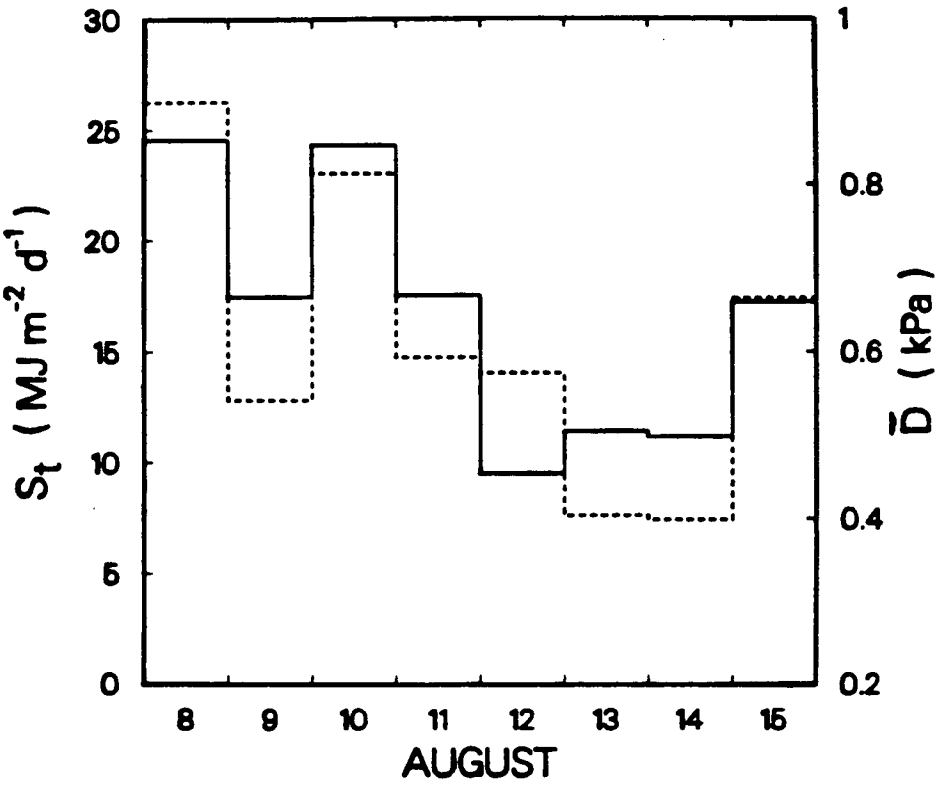

Figure 1.15 Daily total solar irradiance measured above the tree canopy (S_t(——)) and daily average vapour pressure deficit measured below the canopy ($\bar{D}$(-----)) for the period August 8-15, 1984.

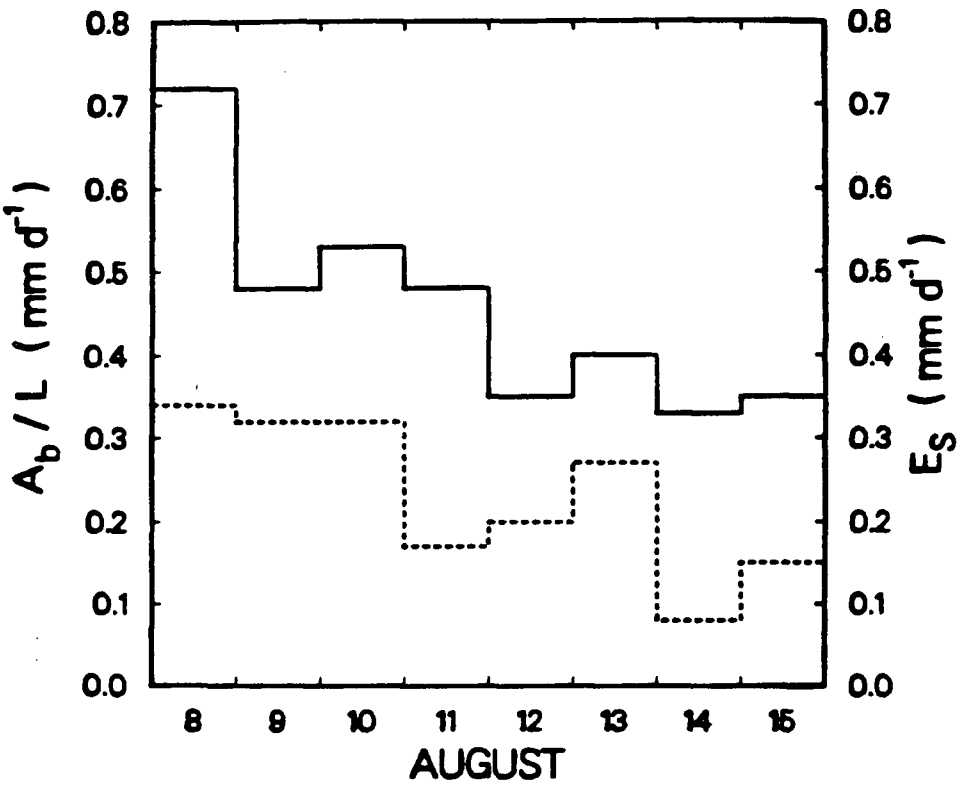

Figure 1.16 Daily below canopy available energy flux density expressed as equivalent water evaporated (A_b/L (——)) and daily forest soil evaporation (E_s(-----)) for the period August 8-15, 1984.

first three measurement days, with 47-65% of A_b going into latent heat flux. While A_b and the average atmospheric vapour pressure deficit ($\bar{D}$) were similar on August 9 and 11, E_s on August 11 was less by almost 50%. The higher rate of evaporation on August 9 was likely due to the evaporation of water which infiltrated the surface of the organic layer during the precipitation events recorded on August 5 and 6. The increased A_b and $\bar{D}$ maintained the evaporation rate on August 10 even though the surface resistance to vapour diffusion (r_{co}) was increasing as the surface organic layer dried.

A similar pattern of events was observed on August 13 where the increased evaporation rate appeared to be due to the evaporation of a small amount of water which accumulated on the surface of the organic layer during the precipitation event recorded in the early morning. The following day $\bar{D}$ remained constant, A_b decreased by 15%, and E_s was reduced by 70%. An increase in A_b and $\bar{D}$ on August 15 to levels comparable to those observed on August 12 resulted in similar values for E_s on these two days.

The average volumetric soil water content to a depth of 0.75 m was measured on August 5 and 17, and was found to have decreased from 0.10 to 0.08 $m^3\ m^{-3}$ (Black et al. 1985). The water balance analysis for this period indicated that the average daily evapotranspiration from the stand where salal had been removed was between 1.28 and 1.50 mm of water. The average 24 hr E_s during the measurement period was 0.23 mm of water, which was 15-18% of the whole stand evapotranspiration.

Gravimetric samples of the 0-50 mm organic layer, collected on August 5 and 17, showed that the volumetric water content of the surface

decreased from 0.08 to 0.04 $m^3\ m^{-3}$, which was equivalent to the evaporation of 2 mm of water. The total evaporation recorded by the lysimeter for the 8 day measurement period was 1.85 mm of water.

For similar soil moisture conditions but lower A_b due to higher stand density Plamondon (1972) found that E_s, in a Douglas-fir stand with no understory at the U.B.C. Research Forest at Haney, ranged from 0.1 - 0.15 mm d^{-1}, which was 33-50% of A_b. At higher soil moisture contents he found that 80-100% of A_b went into latent heat flux, which resulted in maximum 24 hr E_s of 0.3 mm d^{-1}. Kelliher (1985) measured E_s, in plots with understory removed in a thinned Douglas-fir stand near Courtenay, B.C., which ranged from 0.6 mm d^{-1} when the root zone water content was high, down to 0.1 mm d^{-1} at low soil water content.

Figure 1.17 shows the change in the forest floor diffusive resistance (r_{co}) from August 8 to 15. Values of r_{co}, which is considered to be the resistance to vapour diffusion resulting from the presence of a thin, dry, surface layer of organic matter, were calculated by rewriting (10) as

$$r_{co} = \frac{\rho c_p D}{\gamma LE} + r_A\left[\frac{s}{\gamma}\left(\frac{(R_n - G)}{LE} - 1\right) - 1\right] \qquad (20)$$

The bulk aerodynamic resistance (r_A) was assumed to be 100 s m^{-1}. Decreasing the estimate of r_A by 50% resulted in a 10% decrease in the computed values for r_{co}. Kelliher (1985) found r_{co} ranged from 800-3400 s m^{-1} for a similar forest floor. Denmead (1984) working in a pinus radiata stand found r_{co} to range between 120 and 1430 s m^{-1}.

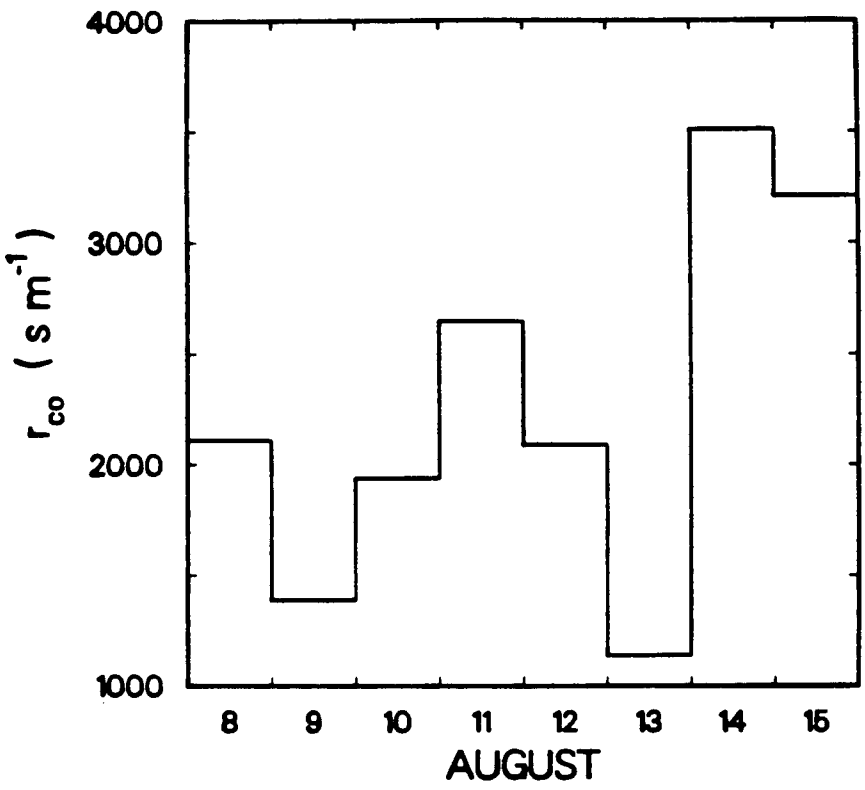

Figure 1.17 Forest floor diffusive resistance (r_{co}) calculated from the rearranged Penman-Monteith equation, for the period August 8-15, 1984.

4.2 Measured Understory Evapotranspiration Rates

The leaf area index (LAI, projected area) of the salal growing in the lysimeter was found to be 1.0. The LAI of the salal within the plot varied between 0.5 and 3.0. New leaves were observed on the salal in the lysimeter, in April 1985, which indicated that the plants had not been damaged in the process of isolating the soil column the previous summer. The stomatal resistance to vapour diffusion (r_s) for salal plants growing within and around the lysimeter was found to be very similar for the period during which lysimetric measurements of understory evapotranspiration were made (Table 1.4). This provided further evidence that the roots of the salal plants in the lysimeter were not excessively damaged when the soil column was isolated, and indicated that the soil moisture conditions they experienced, during the course of the experiment, were not significantly different from the moisture conditions in the soil surrounding the lysimeter.

The average volumetric soil water content of the plot area decreased from 0.11 to 0.08 $m^3\ m^{-3}$ during the period June 26 to July 9. The soil water potential on July 11, measured with the soil psychrometers, indicated that the soil water potential ranged from -0.5 MPa at the 15 cm depth to -0.4 MPa at the 75 cm depth. Interestingly the soil moisture potential in the plot where salal had been removed was found to be the same as where salal was present. No significant precipitation had been recorded for several days prior to June 26, and since the unsaturated hydraulic conductivity of the coarse textured soil was very low, it can be assumed that there was no significant drainage

Table 1.4 Average stomatal resistance of the abaxial surface of salal, growing in and around the lysimeter, measured on 5 days during which the understory evapotranspiration was being measured by the weighing lysimeter

Date	Time (PST)	Average Stomatal Resistance (s m^{-1})	
		Salal in Lysimeter	Salal Outside Lysimeter
June 21	1500	770	670
22	1500	610	510
25	1030	820	840
26	1330	920	900
July 08	1030	1,390	1,340

from the plot, and that the change in volumetric soil water content was due to evapotranspiration. The total stand evapotranspiration, for the period June 26 - July 9, was 24 mm of water or approximately 2 mm d^{-1}.

The tree canopy above the lysimeter containing salal was much less dense than the canopy above the lysimeter in the cleared plot. Figure 1.18 shows the typical (June 26) diurnal trend in above (A_a) and below tree canopy available energy flux density for fine days. The 24 hr A_a was 18.5 MJ m^{-2} d^{-1} and A_b was 5.5 MJ m^{-2} d^{-1}, whereas, for a day with 24 MJ m^{-2} d^{-1} S_t (this is estimated to correspond to a 24hr A_a of 16-18 MJ m^{-2} d^{-1}) measured above the cleared plot, the 24 hr A_b was only 1.7 MJ m^{-2} d^{-1}.

From Figure 1.18 it can be seen that the peak in the evapotranspiration rate (0.11 mm hr^{-1} equivalent to LE = 70 W m^{-2}) coincided with the peak in D. In the morning, while D was low, a period of high A_b only slightly increased the evapotranspiration rate above the night time rate; however, as D increased between 0900 PST and 1200 PST the evapotranspiration rate continued to increase despite a dramatic reduction in A_b.

From 0900 - 1200 PST the latent heat flux density equalled and even exceeded A_b, which required that there be a sensible heat flux from the air to the evapotranspiring surfaces. Since A_b, for this period, was close to zero the supply of relatively warm air must have come from above, which suggests that the air surrounding the salal canopy was well coupled to the atmosphere above the stand. A comparison of D above and below the tree canopy showed that they were virtually the same.

A cumulative plot of evapotranspiration for June 26 is shown in

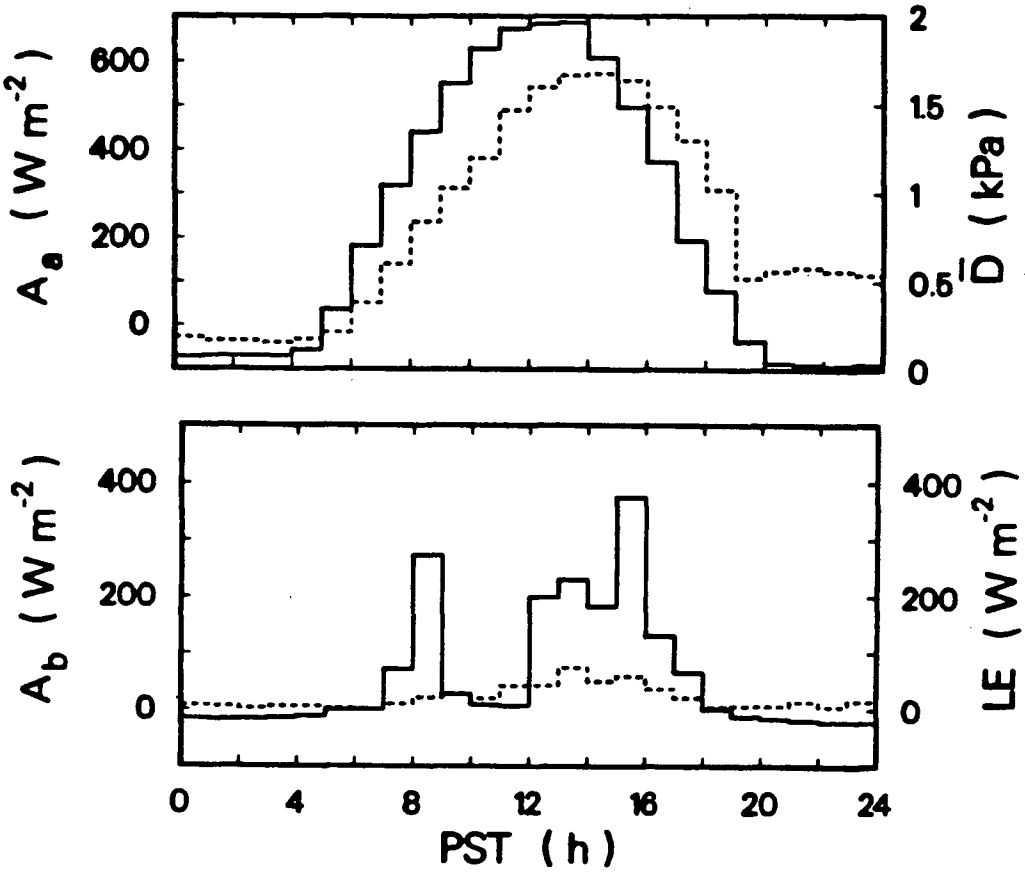

Figure 1.18 Courses of available energy flux density measured above the tree canopy (A_a(——)) vapour pressure deficit and available energy flux density measured below the tree canopy ($\bar{D}$(-----) and A_b(——)), and the measured latent heat flux density from the understory (LE(-----)) for June 26, 1985.

Figure 1.19. The 24 hr total evapotranspiration for days when diurnal measurements were made are presented in Table 1.5, together with the depth of precipitation on the lysimeter, 24 hr total A_a and A_b, and the 24 hr average D measured above the salal canopy. The 24 hr total evapotranspiration varied from 0.63 - 0.84 mm with a mean value of 0.70 mm; however, there was no significant decline in the daily total evapotranspiration during the 17 day measurement period.

The lysimeter recorded 0.14 mm of precipitation between July 4 (2200 PST) and July 5 (0500 PST). Figure 1.20 shows the diurnal trend in A_a, A_b, below tree canopy D, and the corresponding trend in latent heat flux density (LE) from the understory for July 5. The negative LE indicated for the periods 0000 - 0100 PST and 0500 - 0600 PST indicate precipitation on the lysimeter. An increase in D between 0700 and 0800 PST appeared to result in a rapid evaporation of the precipitation intercepted by the salal foliage and the surface of the forest floor organic litter layer. The LE for this period exceeded A_b and was much greater than the LE which was normally observed at that time of the day.

After the intercepted water was evaporated the evapotranspiration rate dropped to a level approaching that which was normally observed for the morning period, however, A_b and D during the early afternoon were substantially lower than on previous days and therefore the evapotranspiration rate was also reduced. An improvement in the weather in the later afternoon resulted in a peak in A_b between 1500 and 1600 PST but D remained low and as a result the evapotranspiration rate did not increase.

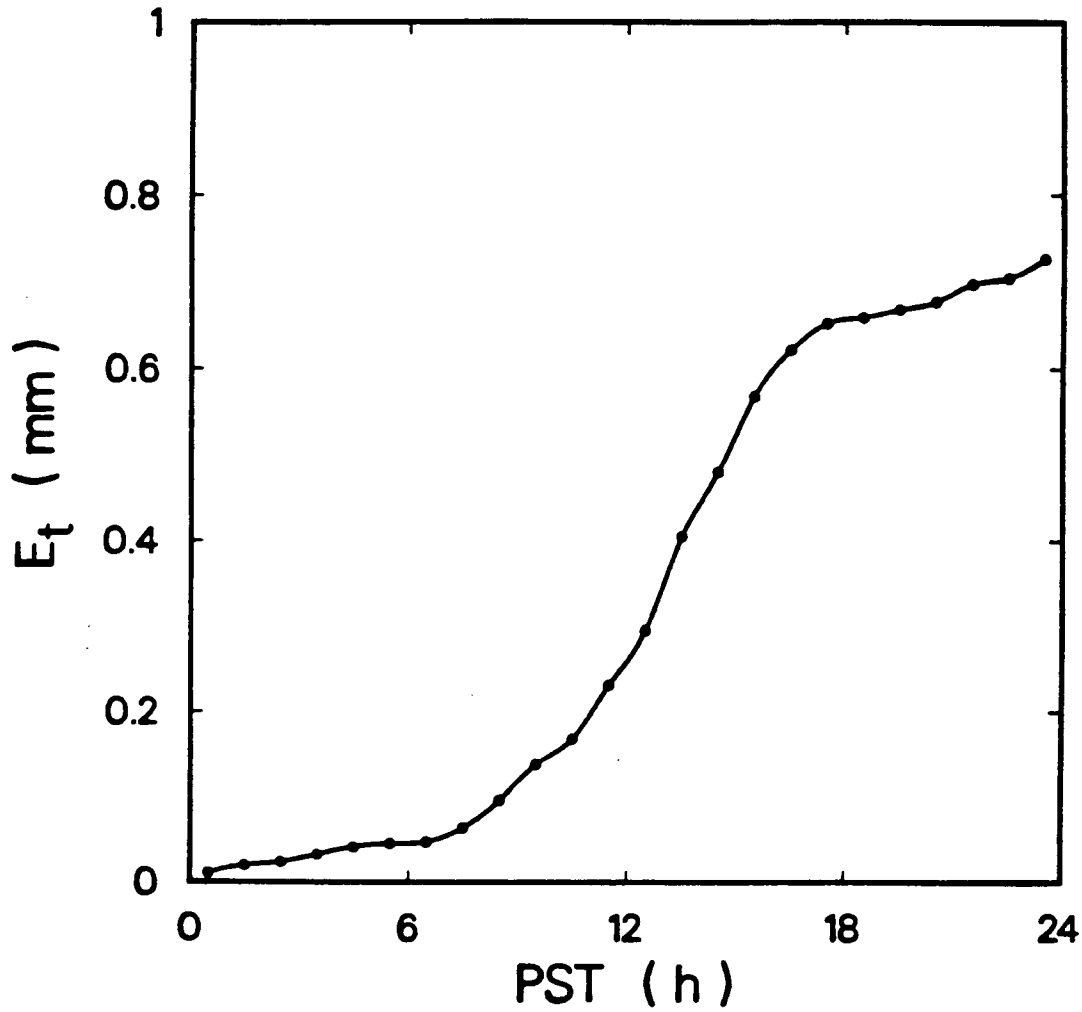

Figure 1.19 Cumulative understory evapotranspiration for June 26, 1985.

Table 1.5 Daily (24 hour) understory evapotranspiration (E_t) for days when diurnal measurements were made; total precipitation (P) on the lysimeter; daily available energy flux density measured above (A_a) and below (A_b) the tree canopy; and daily average vapour pressure deficit ($\bar{D}$) measured below the tree canopy

Date	E_t (mm)	P (mm)	A_a (MJ m^{-2})	A_b (MJ m^{-2})	$\bar{D}$ (kPa)
June 21	0.70	-	19.0	7.7	0.92
22	0.71	-	15.9	6.5	0.60
25	0.68	-	19.7	5.7	0.78
26	0.73	-	18.5	5.5	0.82
July 04	0.84	0.04	-	6.2	1.19
05	0.63	0.10	10.6	4.9	0.52
06	0.60	-	17.4	5.3	0.85
07	0.71	-	17.6	6.2	1.22

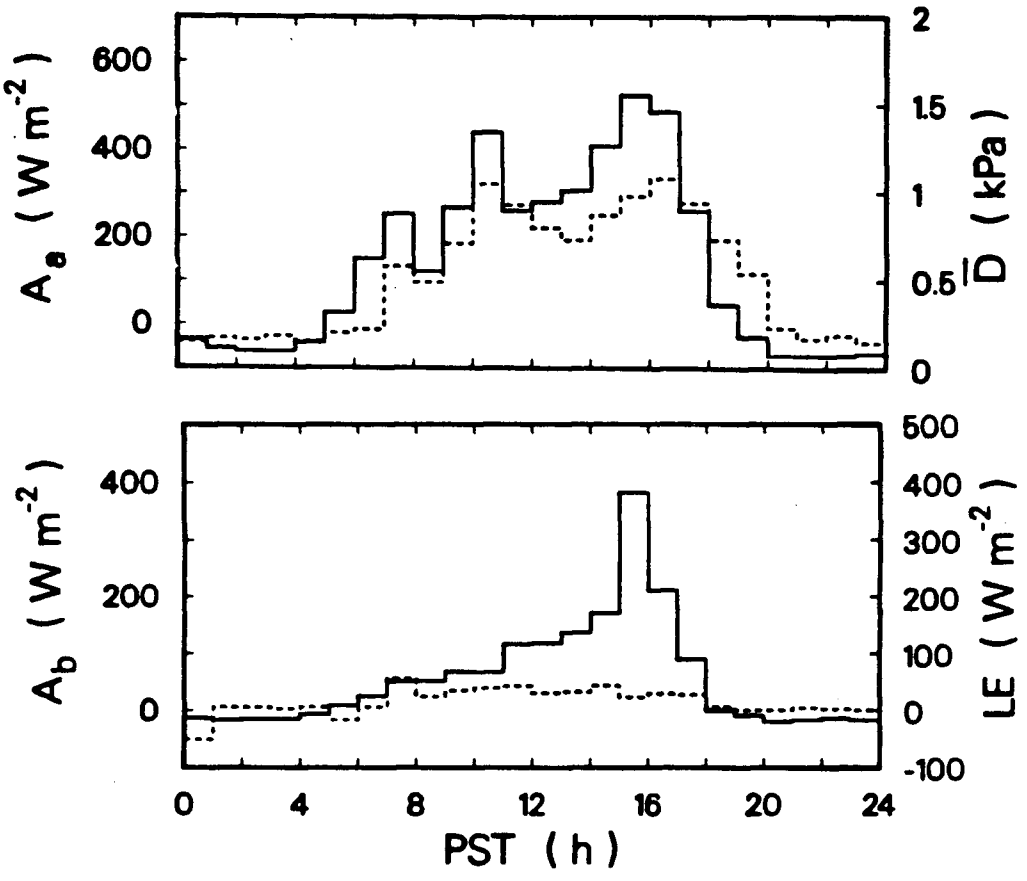

Figure 1.20 Same as for Figure 1.18 except for July 5, 1985.

The fact that the evapotranspiration rate did not increase in response to an increase in A_b on July 5, suggests that the evapotranspiration rate was either soil water supply limited or that it was poorly coupled to A_b. Table 1.6 shows that on a 24 hr basis the evapotranspiration from the lysimeter was between 37 and 54% of the equilibrium evapotranspiration rate (E_{eq}) below the tree canopy, which is given by

$$E_{eq} = [s/(s + \gamma)] \ (Rn - G)/L \qquad (21)$$

The 2 mm d^{-1} average evapotranspiration from the whole stand, for the period June 26 to July 9, was approximately 50% of the 24 hr E_{eq} for the stand. The understory evapotranspiration presented in Table 1.5 was between 30 and 42% of the daily total stand water use.

4.3 Forest Floor Evaporation Rates Following Salal Removal

On July 8 the salal growing in the lysimeter was clipped and E_s was measured for three days (Table 1.7). The weather during the three days was similar to that of the previous measurement days; however, the daily average D on July 9 was greater than had previously been observed. The mean 24 hr E_s was 0.37 mm d^{-1}. This rate was approximately 50% of the mean understory evapotranspiration rate with salal present.

While the salal canopy in the lysimeter was not dense, it is reasonable to assume that removing it would result in a significant increase in the net radiation flux density to the forest floor and an

Table 1.6 Daily (24 hour) average temperature ($\bar{T}$) measured below the tree canopy, daily understory equilibrium evapotranspiration rate (E_{eq}), and the ratio of measured daily understory evapotranspiration to the daily understory equilibrium evapotranspiration rate (E_t/E_{eq})

Date	$\bar{T}$ (°C)	E_{eq} (mm)	E_t/E_{eq}
June 21	15.3	1.89	0.37
22	11.8	1.51	0.47
25	14.5	1.41	0.48
26	14.5	1.36	0.54
July 04	17.4	1.62	0.52
05	14.3	1.20	0.53
06	15.7	1.35	0.44
07	18.9	1.64	0.43

Table 1.7 Daily (24 hour)forest soil evaporation (E_s) following salal removal, daily total available energy flux density measured above (A_a) and below (A_b) the tree canopy, and daily average vapour pressure deficit ($\bar{D}$) measured below the tree canopy

Date	E_s (mm)	A_a (MJ m^{-2})	A_b (MJ m^{-2})	$\bar{D}$ (kPa)
July 09	0.41	17.1	5.6	1.76
10	0.36	14.9	4.7	1.12
11	0.34	20.4	6.0	1.18

increase in soil surface temperature. The top few centimetres of the organic forest floor would also increase in temperature resulting in a significant increase in the saturation vapour pressure of the soil air and the vapour pressure gradient between the vapour source and the atmosphere. Removing the salal would also reduce the aerodynamic resistance to vapour transport due to increased windspeed and more effective penetration by gusts down to the forest floor. The vapour pressure would probably decrease, further increasing the vapour pressure gradient between the vapour source within the soil and the atmosphere. The combined effect of altering the meteorological regime at and close to the forest floor, brought about by removing salal, would appear to be a significant enhancement of the forest soil evaporation rate.

The average r_{co} for the three days was 3530 s m^{-1}. This will be discussed later in the context of E_s under a salal canopy.

4.4 Dependence of the Bulk Aerodynamic Resistance to Vapour Transport from the Salal Canopy on Windspeed and Leaf Area Index

The bulk aerodynamic resistance to vapour transport (r_A) was calculated using data averaged over the first 3 minutes after wetting both surfaces of the salal leaves with a plant mister, and the surrounding salal with a manual fire pump. The water sprayed on the salal leaves was observed to bead up, probably due to the waxy cuticle. Using soap as a surfactant was ruled out because of possible deleterious effects on the leaves. At least 80% of the leaf area appeared to be covered by water, however exact estimates were not possible. The depth

of water on the of salal leaves, computed from the measured increase in lysimeter mass after wetting, was found to be 0.10 ± 0.02 mm, which compares well with Kelliher's (1985) estimate of 0.12 mm for salal canopy storage capacity, and with Spittlehouse and Black's (1982) experimental results of 0.1± 0.03 mm of water. Ten runs were conducted with LAI=1, and four runs were conducted with the leaf area doubled by placing clipped salal stems into the lysimeter.

Figure 1.21 shows the values for r_A, calculated using (12), plotted against the mean windspeed ($\overline{u}$) measured 0.3 m above the salal. The boundary-layer resistances (r_{va}), for salal canopies with leaf area indices of 1 and 2, also shown in Fig. 1.21, were calculated using the relationship

$$r_{va} = [F_s 184(d/\overline{u})^{0.5}]/2LAI \qquad (22)$$

where F_s is a shelter factor (Kelliher 1985; Spittlehouse and Black 1982) assumed to be 1 for LAI=1 and 1.5 for LAI=2 (Jarvis et al. 1976), d is the average diameter of the leaves (0.035 m), and $\overline{u}$ is the average windspeed.

The natural logarithm of r_A is plotted against the natural logarithm of $\overline{u}$ in Figure 1.22. Using linear least squares regression analysis the windspeed dependence of r_A for the salal canopy with LAI=1 was found to be

$$r_A = 25.2\ \overline{u}^{-0.554} \qquad (23)$$

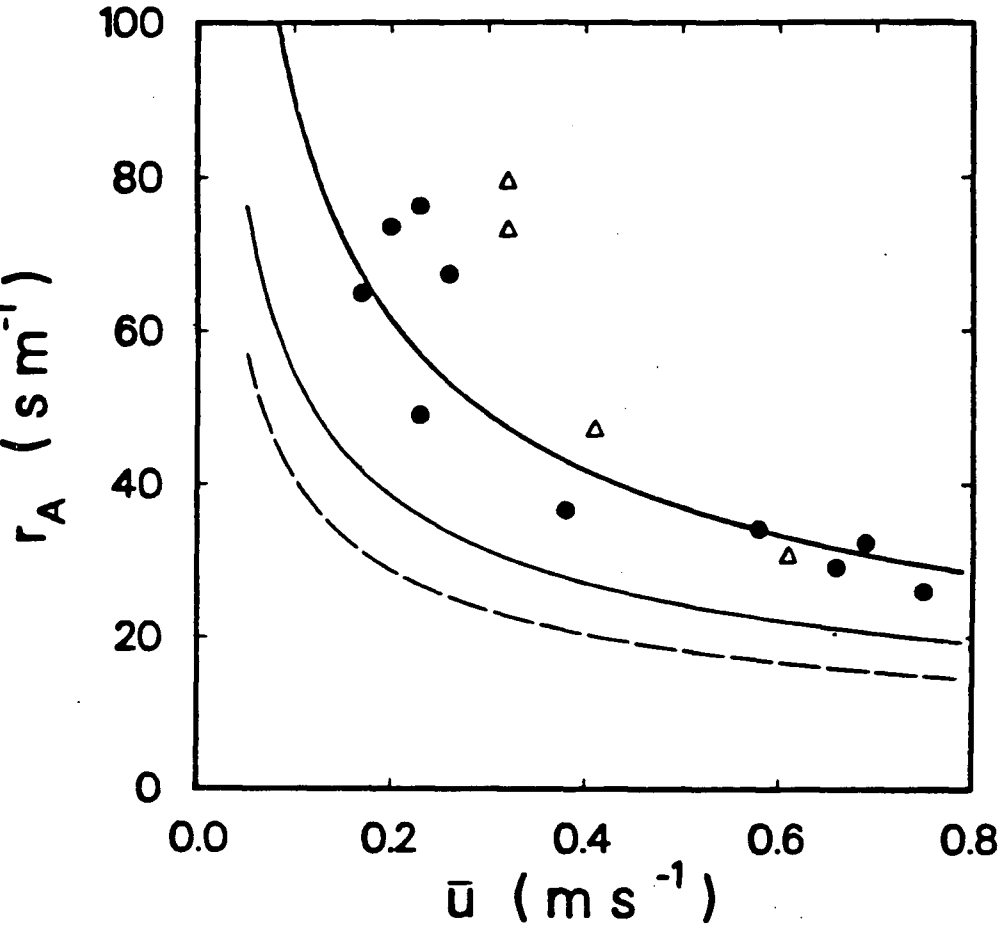

Figure 1.21 Bulk aerodynamic resistance to vapour transport (R_A) from a wet salal canopy to a height of 1.0 m calculated from equation (12) plotted against the mean windspeed ($\bar{u}$) measured 0.3 m above the salal canopy. Values of r_A calculated from data collected with the lysimeter LAI=1 (•) and LAI=2 (Δ). The curve through the data represents the function r_A (s m^{-1}) = 25.2 $\bar{u}^{-0.554}$, ($\bar{u}$ in m s^{-1}), and the two lower curves represent the function $r_{va} = [F_s\ 184(0.035/\bar{u})^{0.5}]/\ 2$ LAI, ($\bar{u}$ in m s^{-1}), where the shelter factor equals 1.0 for LAI=1 (——) and 1.5 for LAI=2 (-----).

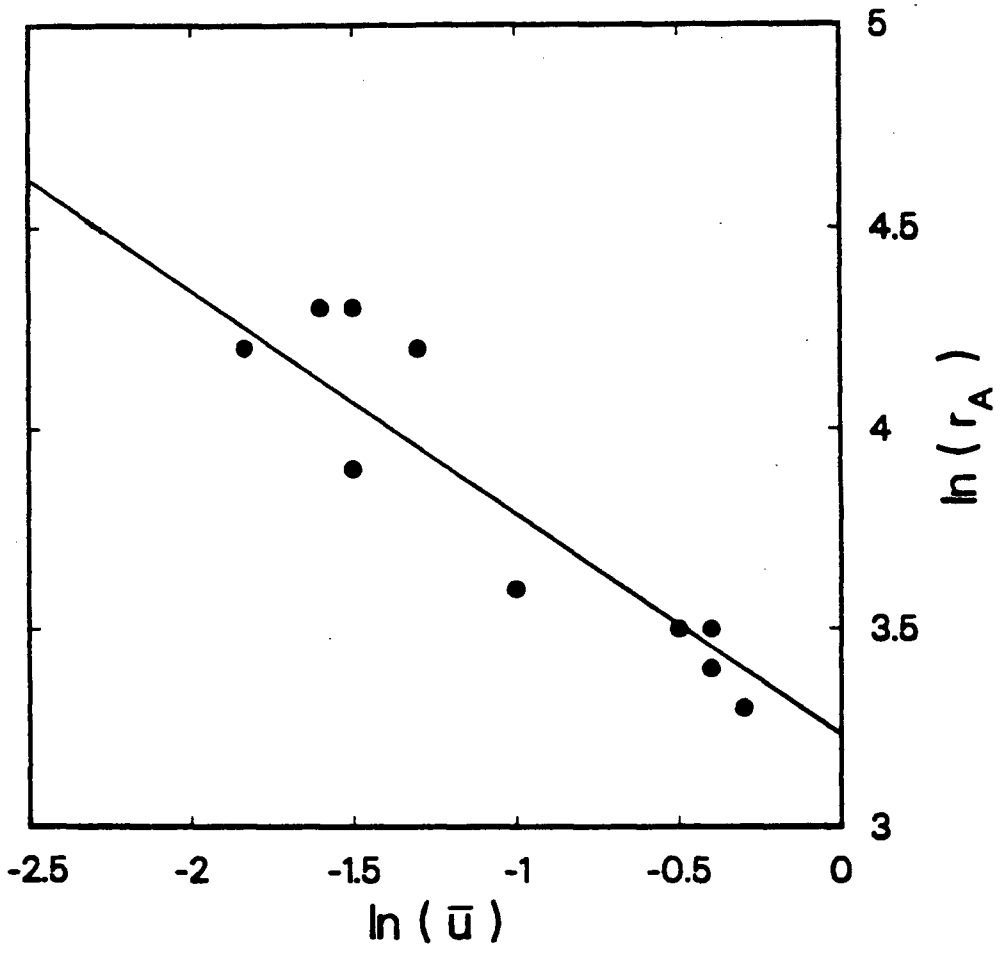

Figure 1.22 The natural logarithm of the bulk aerodynamic resistance to vapour transport (r_A) calculated from equation (12) plotted against the natural logarithm of the mean windspeed ($\bar{u}$).

where r_A is in s m^{-1} and $\bar{u}$ is in m s^{-1}. Equation (23) is plotted as a heavy solid line through the data in Figure 1.21. The fact that the power in (23) is similar to 0.5 suggests that the bulk of the resistance is leaf boundary-layer resistance.

Calder et al. (1984) found that the windspeed dependence of r_A for an upland heather canopy was well described by the function $r_A = (20 \pm 2)\ \bar{u}^{-(0.6 \pm 0.06)}$, which is very similar to (23).

Black et al. (1982) found that the windspeed within a salal canopy with a LAI=3 was 50% of that measured above the canopy. If the windspeed within a sparser canopy (LAI=1) is assumed to be 80% of that measured above the canopy then 70-75% of r_A is attributable to r_{va}. Increasing the LAI to 2 resulted in a reduction in the mean leaf boundary-layer resistance and an apparently more rapid increase in r_A at windspeeds below 0.5 m s^{-1}.

4.5 Applying the Penman-Monteith Equation to the Salal Canopy

Hourly estimates of salal transpiration (E') were calculated using the Penman-Monteith equation (6) to test how well it would estimate salal transpiration under the stand canopy. The canopy resistance values used in the calculations were based on hourly stomatal resistance measurements made on salal leaves surrounding the lysimeter. The bulk aerodynamic resistance was computed using (23).

To use (6) the latent heat flux from the forest soil below the salal canopy is required. E_s was computed using (10), and reasonable

estimates of the differences in the values of meteorological parameters above and below the salal canopy, as illustrated in the following example for 1200 - 1300 PST on June 25.

The average r_{co} for July 9-11, after salal removal mentioned earlier, was 3530 s m^{-1}. This value was used for the forest floor surface resistance in (10). The net radiation flux density below the salal canopy was estimated to be 140 W m^{-2}, i.e., 60% of that measured above the salal. This estimate was based on a leaf area based net radiation flux density extinction model presented by Tanner and Jury (1976). The air temperature was reduced from 23 to 20°C, the vapour pressure was increased from 1.2 to 1.4 kPa, the aerodynamic resistance to sensible and latent heat fluxes from the soil surface to the salal canopy was assumed to be approximately 40 s m^{-1}. For this combination of meteorological parameters E_s was estimated to be 0.01 mm h^{-1}, which was slightly greater than 10% of the measured understory evapotranspiration for this period.

The resulting calculations of salal understory transpiration rates for 0900 - 1600 PST and 1000 - 1700 PST on June 22 and 25 respectively, are presented in Table 1.8. The calculated salal transpiration (E') for June 22 was found to be 8% less than the total measured evapotranspiration minus the 10% assumed to be attributable to E_s, and on June 25, E' was overestimated by 10%.

Table 1.9 shows the effect of altering the assumptions about the ratio of E_s to E_t on E'. Assuming E_s = 0 resulted in E' being underestimated by 20% on June 22 and overestimated by 3% on June 25. At

Table 1.8 Hourly measured understory evapotranspiration (E_t) and calculated salal transpiration (E') for June 22 and 25, 1985

	June 22		June 25	
Time (PST)	E_t (mm h^{-1})	E' (mm h^{-1})	E_t (mm h^{-1})	E' (mm h^{-1})
0900 - 1000	0.05	0.05	-	-
1000 - 1100	0.04	0.04	0.02	0.04
1100 - 1200	0.07	0.06	0.05	0.05
1200 - 1300	0.14	0.11	0.06	0.07
1300 - 1400	0.09	0.07	0.08	0.07
1400 - 1500	0.08	0.06	0.07	0.07
1500 - 1600	0.09	0.07	0.09	0.08
1600 - 1700	-	-	0.06	0.06

Table 1.9 The effect of altering the assumption about the amount of forest soil evaporation that occurred, while the salal canopy was present, on the calculation of salal transpiration

E_s/E_t	$E'/(E_t - E_s)$	
	June 22	June 25
0.0	0.8	1.03
0.1	0.92	1.10
0.2	1.02	1.17
0.5	1.18	1.30

the other extreme, assuming E_s was equivalent to that measured when no salal was present, i.e., 50% of the measured understory evapotranspiration, resulted in E' being overestimated by 18-30%.

Tan et al. (1978) computed salal transpiration using the following approximation

$$E = \frac{\rho c_p}{L\gamma} \frac{D}{r_s} \tag{24}$$

They noted that the salal leaves were generally 1-2°C warmer than air temperature and that E computed using D would be underestimated, however, they felt that this would be offset by not including the boundary-layer resistance to latent heat flux. Calculating salal transpiration using (24) for June 22 and 25 resulted in 25% and 5% underestimates of the measured rates for the two days respectively, assuming that 10% of the measured understory evapotranspiration was due to E_s.

The effect of windspeed on transpiration is complicated by the fact that $1/r_A$ appears in both the numerator and the denominator of (6). Monteith (1965) has shown that the transpiration rate will be independent of windspeed when the canopy resistance to vapour flux equals a critical resistance given by

$$r_c^* = [\rho c_p (1 + \gamma/s) D] / \gamma(Rn - G) \tag{25}$$

Grace (1977) presented experimental evidence demonstrating that at high rates of energy absorption an increase in windspeed causes a decrease in the surface temperature and a reduction in the transpiration rate. If the canopy resistance is less than the critical resistance the transpiration rate will increase in response to increased windspeed.

The hourly average canopy resistance and computed critical resistances for June 22 and 25 are presented in Table 1.10. The canopy resistance was generally much greater than r_c^*; however, during the two hours from 1000 - 1200 PST on June 25, A_b was very low and the computed r_c^* was similar to the measured canopy resistances. During the day, when A_b is large, increased windspeed will tend to reduce the transpiration rate of salal.

Use of the Penman-Monteith equation to estimate understory transpiration requires estimates of $\bar{u}$ below the tree canopy. Generally $\bar{u}$ below the tree canopy was found to be within 6-15% of $\bar{u}$ above the trees; however, there is a good deal of scatter in the relationship which is not unexpected in view of the complexity of turbulent transport in the tree canopy.

Monteith (1965) demonstrated that the relative transpiration rate, written as

$$\frac{E_d}{E_w} = \frac{s + \gamma}{s + \gamma(1 + r_c/r_A)} \qquad (26)$$

or

Table 1.10 Hourly measured canopy resistances and computed critical canopy resistances for June 22 and 25, 1985

	June 22		June 25	
Time (PST)	r_c (s m^{-1})	r^*_c (s m^{-1})	r_c (s m^{-1})	r^*_c (s m^{-1})
0900 - 1000	546	266	-	-
1000 - 1100	594	287	865	766
1100 - 1200	505	251	787	1,008
1200 - 1300	554	61	787	176
1300 - 1400	510	126	767	183
1400 - 1500	405	188	767	202
1500 - 1600	535	90	753	115
1600 - 1700			759	186

$$\frac{E_d}{E_w} = [1 + (\frac{\gamma}{s + \gamma}) \frac{r_c}{r_A}]^{-1}$$

where E_w is the evaporation rate from wet foliage and E_d is the transpiration rate from dry foliage under the same meteorological conditions, depends only on the air temperature and the ratio of r_c to r_A. The average relative transpiration rate for salal during June 22 and 25 was found to be 0.19. The average relative transpiration rate calculated from the lysimeter measurements made immediately before, during, and after the wetting experiments was 0.21. This compares with an average relative rate of 0.19, calculated using (26), for the meteorological conditions prevalent during the canopy wetting experiments and assuming that the stomatal resistance was similar to that which was measured on salal surrounding the lysimeter.

4.6 The Relative Importance of Net Radiation and Vapour Pressure Deficit in Determining the Latent Heat Flux Density from the Salal Canopy

McNaughton and Jarvis (1983) rearranged the Penman-Monteith equation, in order to show explicitly the equilibrium or radiative term and the advective term, as follows:

$$LE = \frac{s}{s + \gamma} (Rn - G) + \frac{\rho c_p (D - D_{eq})}{(s + \gamma) r_A + \gamma r_c} \qquad (27)$$

where D_{eq} (the equilibrium vapour pressure deficit) is given by

$$D_{eq} = \frac{s}{(s + \gamma)} \frac{\gamma r_c}{\rho c_p} (Rn - G) \qquad (28)$$

The equilibrium vapour pressure deficit can be interpreted as being the vapour pressure deficit required to obtain a latent heat flux, across an existing canopy resistance, which is equal to the equilibrium evaporation rate for a given available energy flux density. As r_c increases there is an increase in the ratio of sensible to latent heat flux density which results in warming of the air above the exchange surface. As the air warms D increases and given sufficient time it will increase until it equals D_{eq} and the evaporation rate equals the equilibrium evaporation rate. Finnegan and Raupach (1985) demonstrate that there may not be time for this to happen because the quiescent periods between penetrating gusts of air from above the forest canopy are at best 3 minutes long.

The measured canopy resistance of the salal around the lysimeter was quite large, and consequently, D_{eq} exceeded the measured D whenever the available energy flux density was much greater than 50 W m^{-2}. This resulted in the advective term in (27) becoming negative, which, when combined with the observation that D above the salal was similar to D above the trees, suggests that there was a high rate of exchange between the atmosphere above the salal canopy and the atmosphere above the tree crowns. Furthermore, the atmosphere above the trees is well coupled to the atmosphere in the well mixed portion of the planetary boundary-layer, and therefore the vapour pressure deficit above the trees is determined by regional advective processes. Since D

above the salal was maintained, through effective turbulent mixing, at a level below D_{eq} for the salal canopy it appears that there was advective depression of the evaporation rate.

McNaughton and Jarvis (1983) also presented the Penman-Monteith equation in a form which included a factor (Ω) that gives the relative importance of the equilibrium term and a term that represents the transpiration rate that would occur if the vapour pressure deficit in the outer portion of the planetary boundary-layer were imposed at the surface with no local adjustment, as follows

$$LE = \Omega\left(\frac{s}{s + \gamma}\right)(R_n - G) + (1 - \Omega)\left(\frac{\rho c_p D_m}{\gamma r_c}\right) \qquad (29)$$

where

$$\Omega = \left[1 + \left(\frac{\gamma}{s + \gamma}\right)\left(\frac{r_c}{r_{as}}\right)\right]^{-1}, \qquad (30)$$

D_m is the vapour pressure deficit at a reference height in the well mixed portion of the planetary boundary-layer, and r_{as} is the aerodynamic resistance to vapour flux from the exchange surface to the reference height within the planetary boundary-layer. From (30) it can be seen that Ω is determined by the ratio of r_c to r_{as}.

Equations (29) and (30) can be used to describe the degree of coupling of salal transpiration to the available energy flux density and vapour pressure deficit below the Douglas-fir canopy. This requires that r_{as} in (30) be replaced by r_A, and D_m in (29) by D. With

this change, it can be seen by comparing (30) and (26) that Ω for the salal understory is equal to its relative transpiration rate (E_d/E_w), which was found to be approximately 0.2. This indicates that the advective term in (29) is the dominant term. Since D above the salal was very similar to that above the tree canopy, this analysis shows that the evapotranspiration rate is responding to the imposition of the regional vapour pressure deficit at the salal canopy with essentially no local adjustment.

As part of the derivation of (29) and (30), McNaughton and Jarvis (1983) showed that the vapour pressure deficit at the surface is given by

$$D_o = \Omega D_{eq} + (1 - \Omega) D_m \qquad (31)$$

In this case Ω establishes the relative importance of the available energy flux density at the surface and turbulent mixing above the surface in determining the vapour pressure deficit immediately above the exchange surface. When Ω is large, the surface is isolated from the planetary boundary-layer by a large aerodynamic resistance and D_o approaches D_{eq}. When Ω is small, due to effective turbulent mixing, then the atmosphere at the exchange surface is coupled to the atmosphere within the well mixed portion of the planetary boundary-layer and D_o approaches D_m. Since D_m is only slowly altered by the underlying surface, D_o becomes a regionally set value controlled by regional advective processes.

The small Ω values computed for the salal canopy indicate that D_o

at the salal leaves was controlled by D above the salal canopy. As indicated earlier, the latter was similar to D above the trees. The values of D were substantially less than the vapour pressure deficit which would have existed had the air above the salal canopy been effectively decoupled from the atmosphere above the stand. Stewart (1984) reported a similar result for a bracken fern understory in Thetford Forest, U.K.; however, in that case the humidity deficit above the forest was 8.2 g kg^{-1} and 1.24 m above the ground it was 8.6 g kg^{-1}, whereas, for the 48 W m^{-2} of available energy and the relatively low canopy resistance the equilibrium humidity deficit would have been 1.0 g kg^{-1}. In this case the understory evapotranspiration was being advectively enhanced by the imposition of a regional D which was much greater than D_{eq}. Kelliher (1985) showed that salal understory evapotranspiration was much higher than E_{equil}, thus demonstrating advective enhancement. Again D above the salal was similar to that above the tree canopy; however, low r_c resulted in D being much greater than D_{eq}.

5. CONCLUSION

Two 400 kg weighing lysimeters, with a resolution of 0.006 mm of water, were constructed to measure hourly rates of forest floor evaporation and understory transpiration in a 23-year-old Douglas-fir plantation. The weighing mechanism was an above-ground counterbalanced beam which pivoted on two, 5 cm long, knife edges and was held in suspension by two opposing springs. A linear variable differential transformer resolved changes of 0.01 mm in the vertical displacement of the suspension beam approximately 1.25 m from the fulcrum. Positioning the weighing mechanism above ground simplified construction and minimized the impact on the vegetation surrounding the lysimeter well. The high degree of spatial variability in solar irradiance below the tree canopy caused differential heating of the suspension beam on either side of the fulcrum. This problem was corrected by completely shading the beam from direct solar irradiance.

A technique was developed for isolating undisturbed lysimeter soil columns (0.6 m diameter x 0.75 m deep) containing understory vegetation, without causing significant damage to the plants' root systems. Porometry measurements of the stomatal resistance of salal growing in the lysimeter were found to be similar to those of plants growing outside the lysimeter.

Lysimeter measurements of daily forest soil evaporation rates, following salal removal in a 30 m x 40 m plot, on 8 consecutive days in August 1984, when the soil moisture content was low, ranged from 0.08 -

0.34 mm d^{-1}. These rates were 15-18% of the daily total stand evapotranspiration. In early July 1985, after removing salal from a lysimeter positioned under a less dense tree canopy, the forest soil evaporation rate was found to vary from 0.34 - 0.41 mm d^{-1}, over three days. These forest soil evaporation rates were approximately 50% of the average daily understory evapotranspiration measured on 8 days, out of the previous 17 days, for which daily totals were available. The daily forest soil evaporation was 17-21% of the total stand evapotranspiration.

Forest floor diffusive resistances, computed by rearranging the Penman-Monteith equation, were found to range between 900 and 3500 s m^{-1}. These values are in close agreement with the range of forest floor diffusive resistances reported by Kelliher (1985) for a similar organic forest floor.

The measured daily evapotranspiration rate from a plot with salal understory present was 0.60 - 0.84 mm d^{-1}, which was equivalent to 30-42% of the daily total stand evapotranspiration. Diurnal measurements of hourly evapotranspiration rates were conducted on 8 days when salal was growing in the lysimeter. The maximum hourly evapotranspiration rate observed was 0.13 mm h^{-1}. As much as 10% of the daily total understory evapotranspiration was observed to occur during the night (2000 - 0600 PST).

Utilizing the lysimeter to measure the rate of evaporation from completely wetted foliage proved to be a reliable method for estimating the windspeed dependence of the bulk aerodynamic resistance to vapour

transport. A relationship between r_A (s m^{-1}) and windspeed (m s^{-1}) was found which has the form $r_A = b \bar{u}^m$, where b = 25.2 and m = -0.554 for a salal canopy with LAI=1. Approximately 70-75% of r_A was estimated to be attributable to the leaf boundary-layer resistance, with the remaining 25-30% of the total resistance being due to the resistance of the atmosphere between the salal canopy and the meteorological sensors.

The evaporation rate from wet foliage was found to be 5 times greater than the transpiration rate from dry foliage. This is significant when modelling the evaporation of intercepted precipitation, especially during the growing season when precipitation events are short in duration and often followed by fine weather. Approximately 0.1 mm of water was observed to accumulate on one side of a unit area of leaf.

Using hourly average meteorological measurements, measured stomatal resistance of salal leaves surrounding the lysimeter, and estimates of soil evaporation rate and r_A, as inputs to the Penman-Monteith equation, hourly salal transpiration rates were computed to within 10% of the measured rates ($E_t - E_s$). Since r_A was largely determined by the leaf boundary-layer resistance it has been shown that the Penman-Monteith equation can be used with a reasonable estimate of leaf boundary-layer resistance. This requires windspeed estimates within the salal (in this study windspeed near the salal was 6-15% of that above the stand). The simple vapour diffusion model ($\propto$ LAI D/r_s) was found to underestimate the salal transpiration rate by 5-25%.

For 2 days during which salal leaf stomatal resistance was measured hourly the canopy resistance was generally much greater than the critical resistance at which the latent heat flux density is unaffected by windspeed, and consequently, increased windspeed resulted in a reduction of the latent heat flux.

A range of Ω values between 0.15 and 0.22 were computed for two days during which hourly measurements of r_s were made. The measured understory evapotranspiration was substantially lower than E_{eq} and was found to be largely determined by D. These values of Ω reflect the large r_c relative to r_A. The vapour pressure deficit above the salal canopy was very similar to that above the trees. The D which would have existed above the salal canopy, in the absence of effective turbulent mixing of the atmosphere, i.e. D_{eq}, was found to be much larger than that above the stand. The imposition of the regionally established D on the salal understory resulted in advective depression of the understory evapotranspiration. The lack of local influence on the below tree canopy D suggests that extensive salal removal would not result in an increase in the vapour pressure deficit below the tree canopy.

Mechanically removing salal from a 30 by 40 meter plot required approximately 20 person days of labour. Substantial resprouting was observed to occur during the growing season. The efficacy of currently available herbicides registered for extensive use in forestry projects has not yet been demonstrated for salal control. The operational removal of salal, whether by mechanical or chemical methods, will be an expensive procedure if it is carried out in juvenile stands. This

expense may not be justified in view of the fact that there may only be a 50% reduction in the understory latent heat flux density in response to totally eliminating salal. When the soil surface layers are moist the reduction in latent heat flux density may be even less. Kelliher (1985) reported that salal removal reduced the understory evapotranspiration by 40-60%.

This study tends to support the suggestion by Black and Spittlehouse (1981) that higher stand densities should be maintained on sites which are droughty and have salal as an understory component. In order to keep the understory evapotranspiration rate down to 0.02 mm h^{-1} requires that the below canopy available energy flux density not exceed 20 W m^{-2}; and that the tree canopy be dense enough to prevent efficient mixing of the below canopy air with the air above the trees, so that the dryness of the air surrounding the understory reflects the canopy characteristics and the energy regime of the understory.

With respect to regeneration and stand tending strategies for Douglas-fir stands on droughty sites, the results of this study together with the findings of the other studies reviewed suggest that initial planting densities should be high in order to obtain early crown closure and full site occupancy. Salal growing in shade has reduced leaf area and individual leaves are larger which results in an increased boundary-layer resistance to vapour flux from the leaf (Kelliher 1985).

Thinning operations should be designed to avoid creating large gaps in the tree canopy, as these gaps act like chimneys and increase the ventilation below the tree canopy which results in the maintenance of a

larger atmospheric vapour pressure deficit around the understory vegetation. In order to minimize the number and size of the gaps created in the tree canopy, targeted stand density objectives should be achieved through several light thinning operations rather than a single heavy thinning. The trees removed, during each stand entry, should come from the smaller diameter classes and lower crown positions.

Since the economics of thinning operations are strongly related to the number of times a stand must be entered and the harvestable volume available at each entry, the strategy described above may prove to be economically unacceptable. However, a single heavy thinning is also expensive to conduct and it has been demonstrated that the total productivity of the stand may decline due to the failure of the remaining crop trees to fully exploit the available soil moisture.

The final management option therefore, is to plant at initially high densities, in order to obtain early crown closure, and to allow the stand to self thin through natural mortality. This option, while requiring the least investment, provides the manager with no opportunities for controlling stand development, and no harvestable volume midway through the rotation. For forest firms planning to obtain a significant percentage of their timber supply from thinning operations the loss of mid-rotation harvest opportunities will be costly, especially if replacement timber supplies have to be purchased from the open log market.

BIBLIOGRAPHY

Ainscough, G.L. 1981. The Designed Forest System of MacMillan Bloedel Limited: An example of industrial forest management. The H.R. MacMillan Lectureship in Forestry, U.B.C., Van., B.C.

Anonymous. 1979. Biogeoclimatic Units: Nootka-Nanaimo. B.C. Ministry of Forests, Victoria, B.C.

Anonymous. 1980. Forests and Range Resource Analysis. B.C. Ministry of Forests, Victoria, B.C.

Aston, A.R. 1984. Evaporation from Eucalypts growing in a weighing lysimeter: a test of the combination equations. Agric. For. Meteorol. 31: 241-249.

Black, T.A., C.B. Tanner and W.R. Gardner. 1970. Evapotranspiration from a snap bean crop. Agron. J. 62: 66-69.

Black, T.A., C.S. Tan and J.U. Nnyamah. 1980. Transpiration rate of Douglas-fir trees in thinned and unthinned stands. Can. J. Soil Sci. 60: 625-631.

Black, T.A. and D.L. Spittlehouse. 1981. Modeling the water balance for watershed management. pp. 117-129. In: D.M. Baumgartner (ed.) Proc. Symp. Interior West Watershed Mgt. Apr. 8-10, 1980, Spokane, WA, U.S.A.

Black, T.A., D.L. Spittlehouse, F.M. Kelliher and D.T. Price. 1982. Water balance and management of young Douglas-fir stands. Contract Research Report, E.P. 855, B.C. Min. of For., Victoria, B.C.

Black, T.A., D.T. Price, F.M. Kelliher and P.M. Osberg. 1984. Effect of understory removal on seasonal growth of a young Douglas-fir stand. Contract Research Report, E.P. 855, B.C. Min. of For., Victoria, B.C.

Black, T.A., D.T. Price, P.M. Osberg and D.G. Giles. 1985. Effect of reduction of salal competition on evapotranspiration and growth of early stage Douglas-fir plantations. Contract Research Report to Research Branch, British Columbia Min. of For., Victoria, B.C.

Bradley, E.F., O.T. Denmead and A.W. Thurtell. 1983. Measurements of the turbulence and heat and moisture transport in a forest canopy. Q.J.R. Meteorol. Soc. (in preparation).

Calder, I.R., R.L. Hall, R.J. Harding and I.R. Wright. 1984. The use of a wet-surface weighing lysimeter system in rainfall interception studies of heather (Calluna vulgaris). J. Climate and Appl. Meteorol. 23: 461-473.

Carlson, H. 1974. Springs: Troubleshooting and Failure Analysis. In: W.H. Middendorf (ed.) Engineering Troubleshooting. Vol. 1. Marcel Dekker, Inc., New York.

Daniel, T.W., J. Helms and F.S. Baker. 1979. Principles of Silviculture. Second Edition. McGraw-Hill Book Company. New York.

Denmead, O.T. 1984. Plant physiological methods for studying evapotranspiration: problems of telling the forest from the trees. Agric. Wat. Mgt. 8: 167-189.

Finnegan, J.J. and M.R. Raupach. 1985. Transfer processes in plant canopies in relation to stomatal characteristics. In: E. Zieger, G. Farquar and I. Cowan. (EDS.) Stomatal Function. Stanford Univ. Press, Stanford, CA., U.S.A.

Forest Act. 1979. Available from the Queens Printer for British Columbia, Victoria, B.C.

Fries, J. and S. Hagner. 1970. Economic decision models for silvicultural operations. In: Proceedings silvicultural decison models. American Pulpwood Association, Atlanta, Georgia.

Garratt, J.R. 1984. The measurement of evaporation by meteorologial methods. Agric. Wat. Mat. 8: 99-117.

Gifford, H.H., D. Whitehead, R.S. Thomas and D.S. Jackson. 1982. Design of a new weighing lysimeter for measuring water use by individual trees. N.Z.J. For. Sci. 12: 448-456.

Giles, D.G. 1983. Soil water regimes on a forested watershed. M.Sc. Thesis, Univ. of B.C., Vancouver, B.C.

Grace, J. 1977. Plant Response to Wind. Academic Press, New York, pp. 60-69.

Jackson, D.S., E.A. Jackson and H.H. Gifford. 1983. Soil water in deep Pinaki sands: some interactions with thinned and fertilized Pinus radiata. N.Z.J. For. Sci. 1392: 183-196.

Jarvis, P.G., G.B. James and J.J. Landsberg. 1976. Coniferous forest. pp. 171-240. In: J.L. Monteith (ed.) Vegetation and the Atmosphere. Vol. 2, Case Studies, Academic Press, New York.

Jarvis, P.G., W.R.N. Edwards and H. Talbot. 1981. Models of plant and crop water use. pp. 151-194. In: D.A. Rose and D.A. Charles-Edwards (eds.) Mathematics and Plant Physiology. Academic Press, London.

Kelliher, F.M. 1985. Salal understory removal effects on the soil water regime and tree transpiration rates in a Douglas-fir forest. Ph.D. thesis, Univ. of B.C., Vancouver, B.C.

Klinka, K., F.C. Nuszdorfer and L. Skoda. 1979. Biogeoclimatic units of central and southern Vancouver Island. B.C. Min. of For., Victoria, B.C.

Leverenz, J., J.D. Deans, E.D. Ford, P.G. Jarvis, R. Milne and D. Whitehead. 1982. Systematic spatial variation of stomatal conductance in a Stika spruce plantation. J. Appl. Ecol. 19: 835-851.

McNaughton, K.G. and P.G. Jarvis. 1982. Predicting effects of vegetation changes on transpiration and evaporation. pp. 1-47. In: T.T. Kozlowski (ed.). Water Deficits and Plant Growth, Vol. VII. Academic Press, New York.

Milne, R., J.D. Deans, E.D. Ford, P.G. Jarvis, J. Leverenz and D. Whitehead. 1985. A comparison of two methods of estimating transpiration rates from a Sitka spruce plantation. Boundary-Layer Meteorol. 32: 155-175.

Monteith, J.L. 1965. Evaporation and environment. symp. Soc. Exp. Biol. XIX: 205-234.

Plamondon, A.P. 1972. Hydrologic properties and water balance of the forest floor of a Canadian west coast watershed. Ph.D. thesis, Univ. of B.C., Vancouver, B.C.

Price, D.T., T.A. Black and F.M. Kelliher. 1986. Effects of salal understory removal on photosynthetic rate and stomatal conductance of young Douglas-fir trees. Can. J. For. Res. 16: 90-97.

Raupach, M.R. and B.J. Legg. 1984. The uses and limitations of flux-gradient relationships in micrometeorology. Agric. Water Mgt. 8: 119-131.

Roberts, J., C.F. Pymar, J.S. Wallace and R.M. Pitman. 1980. Seasonal changes in leaf area, stomatal conductance and transpiration from bracken below a forest canopy. J. Appl. Ecol. 17: 409-422.

Roberts, J., R.M. Pitman and J.S. Wallace. 1982. A comparison of evaporation from stands of Scots pine and corsican pine in Thetford Chase, East Anglia. J. Appl. Ecol. 19: 859-872.

Roberts, J., J.S. Wallace and R.M. Pitman. 1984. Factors affecting stomatal conductance of bracken below a forest canopy. J. Appl Ecol. 21: 643-655.

Shuttleworth, W.J. 1978. A simplified one-dimensional theoretical description of the vegetation-atmosphere interaction. Boundary-Layer Meteorol. 14: 3-27.

Shuttleworth, W.J. 1979. Below-canopy fluxes in a simplified one-dimensional theoretical description of the vegetation-atmosphere interaction. Boundary-layer Meteorol. 17: 315-331.

Shuttleworth, W.J. and J.S. Wallace. 1985. Evaporation from sparse crops - an energy balance combination theory. Q.J.R. Meteorol. Soc. 111: 839-855.

Smith, D.M. 1962. The Practice of Silviculture. 7th Edition, John Wiley and Sons, Inc., New York.

Spittlehouse, D.L. and T.A. Black. 1982. A growing season water balance model used to partition water use between trees and understory. pp. 195-214. In: Proc. Can. Hydrol. Symp. 82, Hydrol. processes in for. areas. June 14-15, 1982, Fredericton, N.B.

Stewart, J.B. 1983. A discussion of the relationships between the principal forms of the combination equation for estimating crop evaporation. Agric. Meteorol. 30: 111-127.

Stewart, J.B. 1984. Measurement and prediction of evaporation from forested and agricultural catchments. Agric. Water Mgt. 8: 1-28.

Tan, C.S., T.A. Black and J.U. Nnyamah. 1977. Characteristics of stomatal diffusion resistance in a Douglas-fir forest exposed to soil water deficits. Can. J. For. Res. 7: 595-604.

Tan, C.S., T.A. Black and J.U. Nnyamah. 1978. A simple diffusion model of transpiration applied to a thinned Douglas-fir stand. Ecol. 59: 1221-1229.

Tanner, C.B. 1968. Evaporation of water from plants and soil. pp. 73-106. In: T.T. Kozlowski (ed.) Water Deficits and Plant Growth. Vol. 1. Academic Press, New York.

Tanner, C.B. and W.A. Jury. 1976. Estimating evaporation and transpiration from a row crop during incomplete cover. Agron. J. 68: 239-243.

Thom, A.S. 1971. Momentum absorption by vegetation. Q.J.R. Meteorol. Soc. 97: 414-428.

Thom, A.S. 1975. Momentum, mass and heat exchange of plant communities. pp. 57-109. In: J.L. Monteith (ed.) Vegetation and Atmosphere. Vol. 1, Principles, Academic Press, New York.

Wahl, A.M. 1944. Mechanical Springs. First Edition. Penton Publishing Company, Cleveland, Ohio.

Zahner, R. 1958. Hardwood understory depletes soil water in pine stands. For. Sci. 4: 178-184.

APPENDIX I

Soil Profile Description - Dunsmuir Creek Site

APPENDIX I

Soil Profile Description - Dunsmuir Creek Site

Horizon	Depth (cm)	Description
LF	2-0	Undecomposed and semi-decomposed Douglas-fir needles; abundant very fine and fine horizontal roots; abrupt, smooth boundary; 1 to 3 cm thick.
Ae	0-3	Grayish brown (10 YR 5/2 d) gravelly sandy loam; weak, medium granular; soft; plentiful, fine and medium oblique roots; abrupt, irregular boundary; 2 to 5 cm thick.
Bm1	3-20	Brown (10 YR 4/3 m) gravelly sandy loam; weak, fine subangular blocky; friable; plentiful, fine and medium oblique roots; diffuse, wavy boundary; 15 to 22 cm thick.
Bm2	20-60	Dark yellowish brown (10 YR 4/4 m) gravelly sandy loam; weak, fine subangular blocky; friable; few, fine and medium oblique roots; gradual, wavy boundary; 30 to 50 cm thick.

Horizon	Depth (cm)	Description
BCgc	60-80	Grayish brown (2.5 Y 5/2 m) gravelly loamy sand; common, medium, distinct strong brown (7.5 YR 5/8 m) mottles; massive; firm; very few, very fine oblique roots; discontinuous, weak cementation; clear, wavy boundary; 25 to 40 cm thick.
BCc	88 +	Dark grayish brown (2.5 Y 4/2 m) gravelly sandy loam; massive; extremely firm; no roots; continuous moderate cementation.

Classification: Duric Dystric Brunisol.

Comments: The upper part of the solum apears disturbed by tree-throw and/or logging. Occasional fragments of duric horizon (BCc) were found throughout the Bm horizons.

APPENDIX II

Neutron Probe Calibration Equation

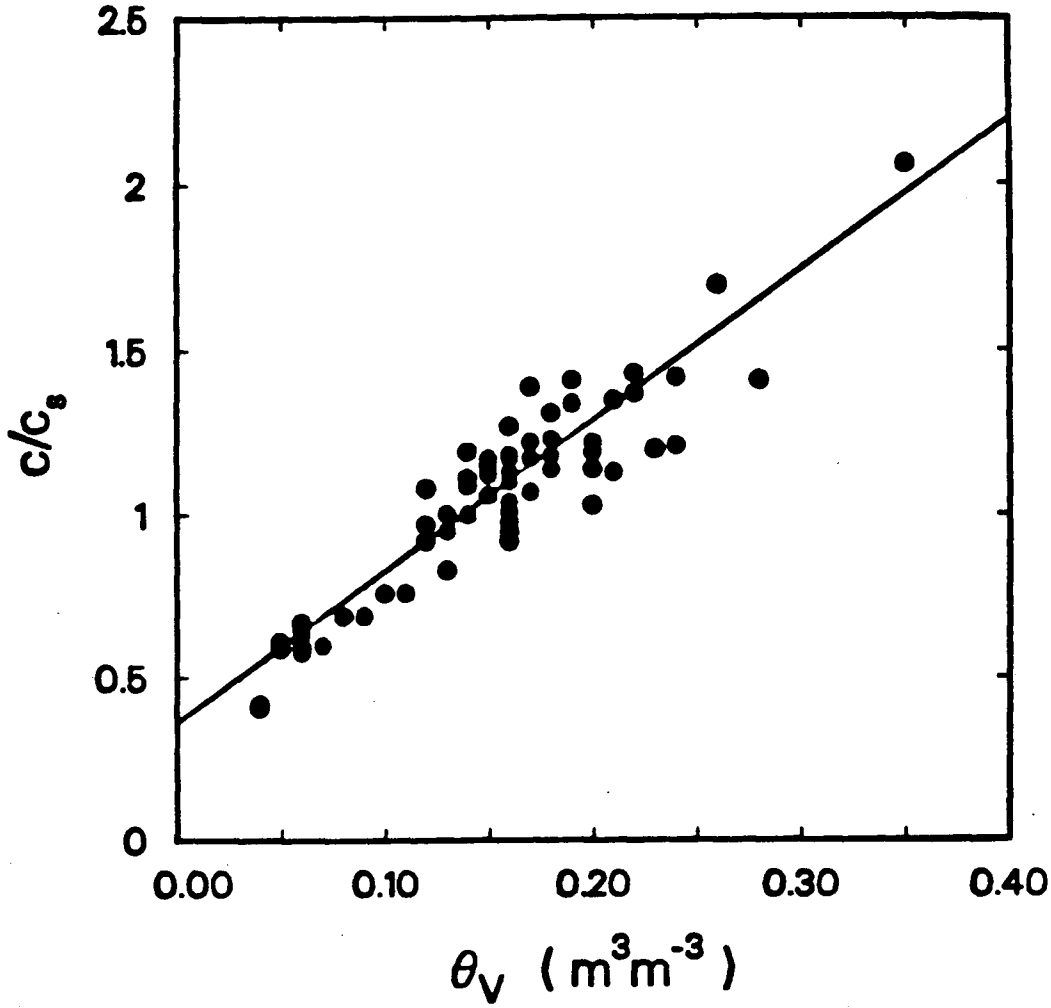

Figure AII.I Neutron probe count ratio (c/c_s) vs vol. soil water content (θ) at the Dunsmuir Creek site. The equation of the repression line is $c/c_s = 0.348 + 4.619\ \theta_v$; $r^2 = 0.88$, Se = 0.11 or $\theta_v = 0.217\ c/cs - 0.075$.

APPENDIX III

Theory of Counteracting Spring Balance

APPENDIX III

Theory of Counteracting Spring Balance

When the lysimeter weighing mechanism is balanced and the suspension beam is level, being held in suspension by two counteracting springs the forces acting rotationally about the fulcrum are given by

$$F_{lys}\, d_{lys} = F_{cw}\, d_{cw} + (F_{BS} - F_{TS})\, d_s \qquad \text{(AIII.1)}$$

where F_{lys} is the force exerted by the mass of the lysimeter, d_{lys} is the length of the suspension beam from the fulcrum to the lysimeter, F_{cw} is the force exerted by the mass of the counterweight, d_{cw} is the length of the suspension beam from the fulcrum to the counterweights, F_{BS} and F_{TS} are the forces exerted by the bottom and top springs, and d_s is the length of the suspension beam from the fulcrum to the point of spring attachment.

If the lysimeter loses some mass through evaporation then the sum of the spring force opposing rotation in the direction of F_{cw} will increase, so that

$$F_{TS} - F_{BS} = k[(X_T + \Delta X_T) - (X_B - \Delta X_B)] \qquad \text{(AIII.2)}$$

however $X_B = X_T$ and ΔX_B (positive for contraction of bottom spring) = ΔX_T (positive for elongation of top spring) = ΔX_s, so

$$F_{BS} - F_{TS} = -2\, k\, \Delta X_s \qquad \text{(AIII.3)}$$

where k is the spring constant (N cm^{-1}), X_T and X_B represents the initial elongation of the top and bottom springs, and ΔX_s is the increase in the elongation of the top spring as a result of a decrease in lysimeter mass.

Substituting (AIII.3) into (AIII.1) gives

$$F_{lys}\ d_{lys} = F_{cw}\ d_{cw} - 2k\ \Delta X_s\ d_s \qquad \text{(AIII.4)}$$

and, therefore,

$$\Delta X_s = \frac{F_{cw}\ d_{cw} - F_{lys}\ d_{lys}}{2k\ d_s} \qquad \text{(AIII.5)}$$

Since $\frac{\Delta X_{LVDT}}{\Delta X_s} \approx \frac{d_{LVDT}}{d_s}$, where ΔX_{LVDT} is the increase in the displacement of the LVDT probe, and d_{LVDT} is the length of the suspension beam from the fulcrum to the LVDT, then to obtain ΔX_{LVDT} for a given ΔF_{lys} requires that (AIII.5) be multiplied by d_{LVDT}/d_s to give

$$\Delta X_{LVDT} = \frac{(F_{cw}\ d_{cw} - F_{lys}\ d_{lys})\ d_{LVDT}}{2k\ d_s^2} \qquad \text{(AIII.6)}$$

If $d_{cw} = d_{lys}$, then

$$\Delta X_{LVDT} = \frac{(F_{cw} - F_{lys})\ d_{lys}\ d_{LVDT}}{2k\ d_s^2} \qquad \text{(AIII.7)}$$

If $d_s = d_{LVDT}$, then

$$\Delta X_{LVDT} = \frac{(F_{cw} - F_{lys})\, d_{lys}}{2k\, d_s} \qquad \text{(AIII.8)}$$

If $d_{lys} = d_s$, then

$$\Delta X_{LVDT} = \frac{F_{cw} - F_{lys}}{2k} \qquad \text{(AIII.9)}$$

At balance, $V_{LVDT} = V_{BAL}$, i.e., $\Delta X_{LVDT} = 0$, where V_{LVDT} and V_{BAL} are the output voltages of the LVDT when the weighing mechanism is in operation and balanced. As the lysimeter loses mass, F_{cw} becomes greater than F_{lys}, ΔX_{LVDT} increases, i.e., $E_t \propto \frac{\Delta X_{LVDT}}{\Delta t}$, and

$$V_{LVDT} = V_{BAL} + b\, \Delta X_{LVDT} \qquad \text{(AIII.10)}$$

where b is the LVDT calibration factor (mv mm^{-1}). Substituting (AIII.10) into (AIII.6) gives

$$\frac{V_{LVDT} - V_{BAL}}{b} = \frac{(F_{cw}\, d_{cw} - F_{lys}\, d_{lys})\, d_{LVDT}}{2k\, d_s^2} \qquad \text{(AIII.11)}$$

which can be rearranged to give F_{lys} as follows

$$F_{lys} = \frac{F_{cw}\, d_{cw}}{d_{lys}} - \left(\frac{2k\, d_s^2}{d_{LVDT}\, d_{lys}}\right)\left(\frac{V_{LVDT} - V_{BAL}}{b}\right) \qquad \text{(AIII.12)}$$

Differentiating F_{lys} with respect to V_{LVDT} yields

$$\Delta F_{lys} = -\left(\frac{2k\ d_s^2}{b\ d_{LVDT}\ d_{lys}}\right) \Delta V_{LVDT} \qquad \text{(AIII.13)}$$

ΔF_{lys} can also be written in terms of the change in the depth of water in the lysimeter as follows

$$\Delta F_{lys} = \pi\ r^2\ \Delta W_d\ \rho_w \qquad \text{(AIII.14)}$$

where r is the radius of the lysimeter, ΔW_d is the depth of water evapotranspired, and ρ_w is the density of liquid water, therefore,

$$\Delta W_d = -\left(\frac{2\ k\ d_s^2}{b\ d_{LVDT}\ d_{lys}}\right) \frac{\Delta V_{LVDT}}{\pi\ r^2\ \rho_w} \qquad \text{(AIII.15)}$$

When ΔW_d is negative evaporation is occurring, i.e., $\Delta V_{LVDT} > 0$ and V_{LVDT} is increasing.

The lysimeter balance calibration factor (mm mV^{-1}) (reciprocal of sensitivity) is obtained by rearranging (AIII.15) to give

$$\frac{\Delta W_d}{\Delta V_{LVDT}} = -\frac{2\ k\ d_s^2}{b\ d_{LVDT}\ d_{lys}\ \pi\ r^2\ \rho_w} \qquad \text{(AIII.16)}$$

The temperature sensitivity of the counteracting springs is related to the difference in elongation between the springs so that when the weighing mechanism is in a balanced or neutral condition both springs

are elongated equally and the effect of temperature on the modulus of rigidity for each spring is the same, and consequently, there are no changes in the relative forces acting on the suspension beam (Carlson 1974; Wahl 1944).

The depth of water in the lysimeter is given by:

$$W_{d1} = W_{ref} - k' \, (1 - m(T - T_o)) \, (V_{LVDT} - V_{BAL}) \qquad \text{(AIII.17)}$$

where W_{ref} is an initial reference depth of water in the lysimeter, T_o is the temperature when the lysimeter was balanced, T is the temperature during the period when weight changes are being measured, m is the temperature sensitivity of the modulus of rigidity for the two springs and

$$k' = \frac{2 \, k \, d_s^2}{b \, d_{LVDT} \, d_{lys} \, \pi \, r^2 \, \rho_w}.$$

The depth of water remaining in the lysimeter after a period during which evaporation was taking place is given by

$$W_{d2} = W_{d1} + \Delta W_d \qquad \text{(AIII.18)}$$

Differentiating ΔW_d with respect to temperature and voltage gives

$$\Delta W_d = \left(\frac{\partial \Delta W_d}{\partial T}\right) \Delta T + \left(\frac{\partial \Delta W_d}{\partial V}\right) \Delta V \qquad \text{(AIII.19)}$$

therefore

$$\frac{\partial \Delta W_d}{\partial T} = k'm \, (V_{LVDT} - V_{BAL}) \qquad \text{(AIII.20)}$$

and

$$\frac{\partial \Delta W_d}{\partial V} = - k' \ (1 - m(T - T_o)) \qquad \text{(AIII.21)}$$